Fundamentals of X-ray interaction with matter

Sang-Kil Son
CFEL-DESY Theory Division
Center for Free-Electron Laser Science, DESY, Hamburg, Germany

---

DESY Summer Student Lectures 'Photon Science'
August 2 and 3, 2021

HELMHOLTZ
RESEARCH FOR GRAND CHALLENGES

CFEL SCIENCE

Center for Free-Electron Laser Science
CFEL is a scientific cooperation of the three organizations:
DESY – Max Planck Society – University of Hamburg

DESY.

Outline

- First day (August 2, 2021)
  - Introduction
  - Theory of X-ray–matter interaction
  - X-ray absorption
  - X-ray atomic physics on computer: XATOM
- Second day (August 3, 2021)
  - X-ray fluorescence
  - Auger-Meitner decay
  - X-ray scattering
  - Computer simulations with XATOM

What is X-ray?

X-ray is…

- discovered by Wilhelm Röntgen in 1895
- photon energy: 100 eV ~ 100 keV
- wavelength: 0.01 nm to 10 nm
- penetrability
- element selectivity

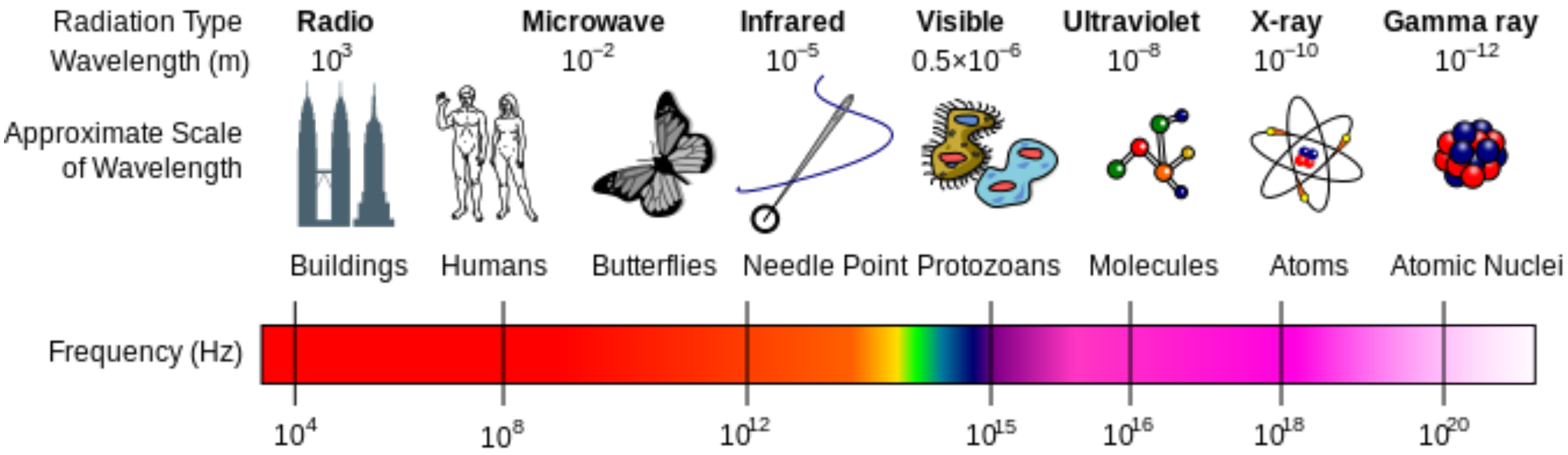

X-ray absorption

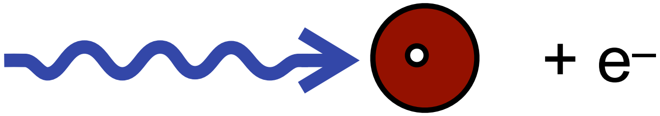

Radiography: see inside due to X-ray absorption contrast

Hand with rings: Röntgen’s first medical X-ray in 1895 (Nobel prize in 1901)

X-ray fluorescence

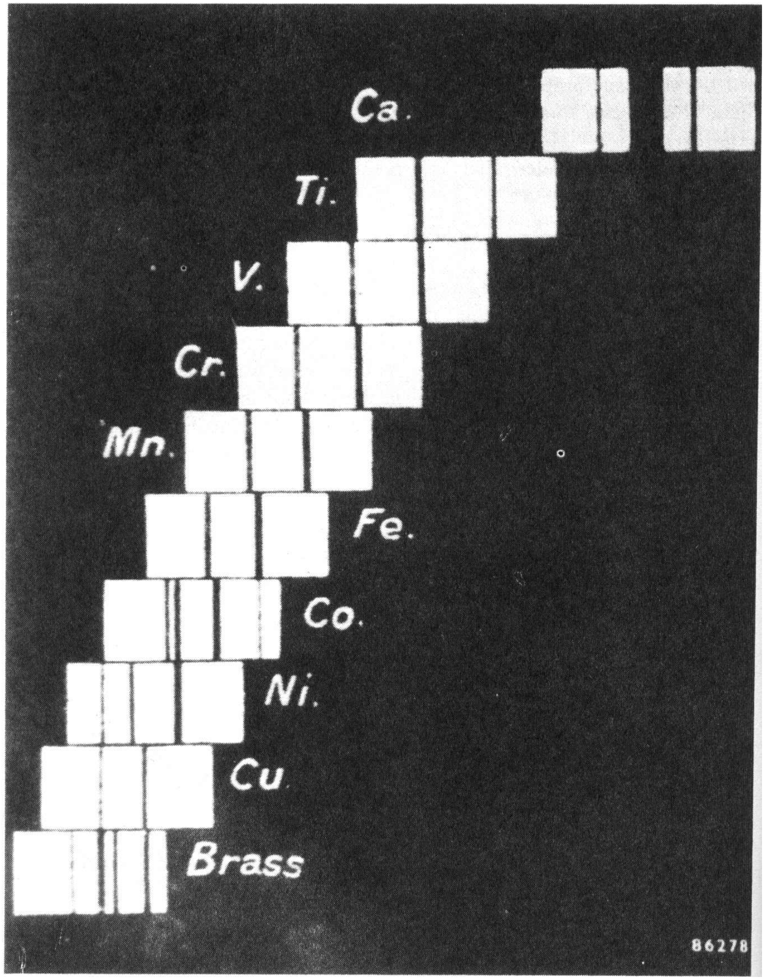

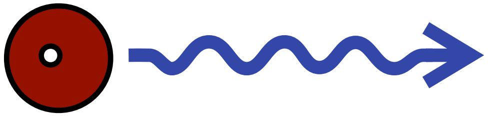

Different chemical compositions identified by X-ray fluorescence

Chemical analysis of elements: First qualitative X-ray chemical analysis by Henry Moseley, *Phil. Mag.* **26**, 1024 (1913).

X-ray scattering / diffraction

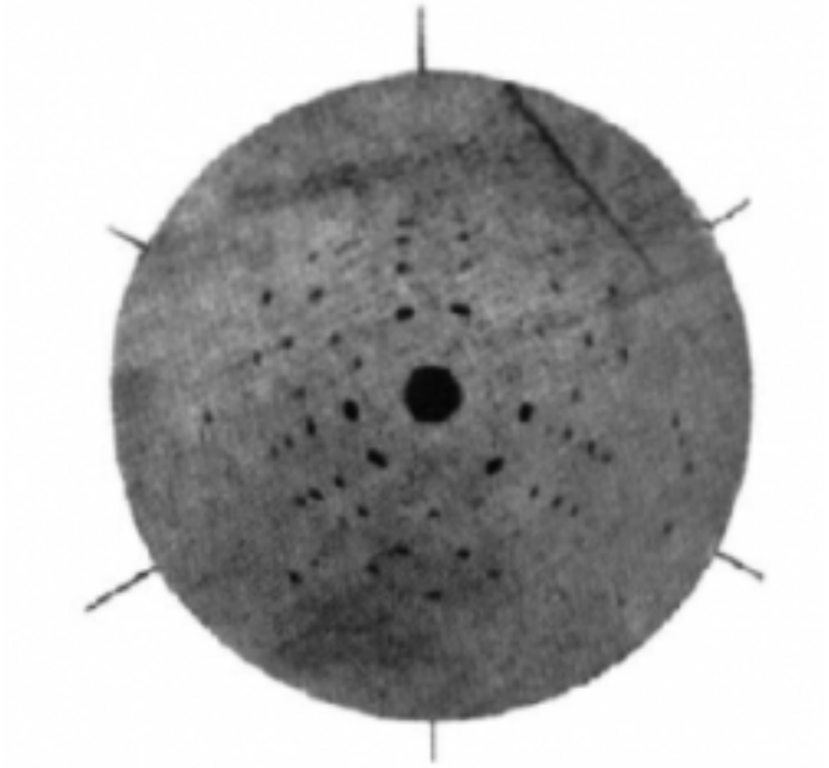

Zinc blend: First published diffraction pattern of a crystal by Max von Laue in 1912 (Nobel prize in 1914)

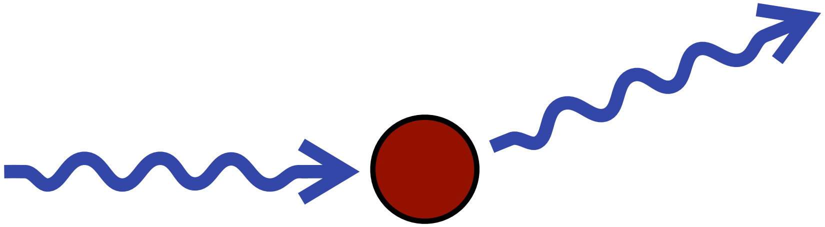

Elastic X-ray scatterings from a crystal make a diffraction pattern.

X-ray crystallography

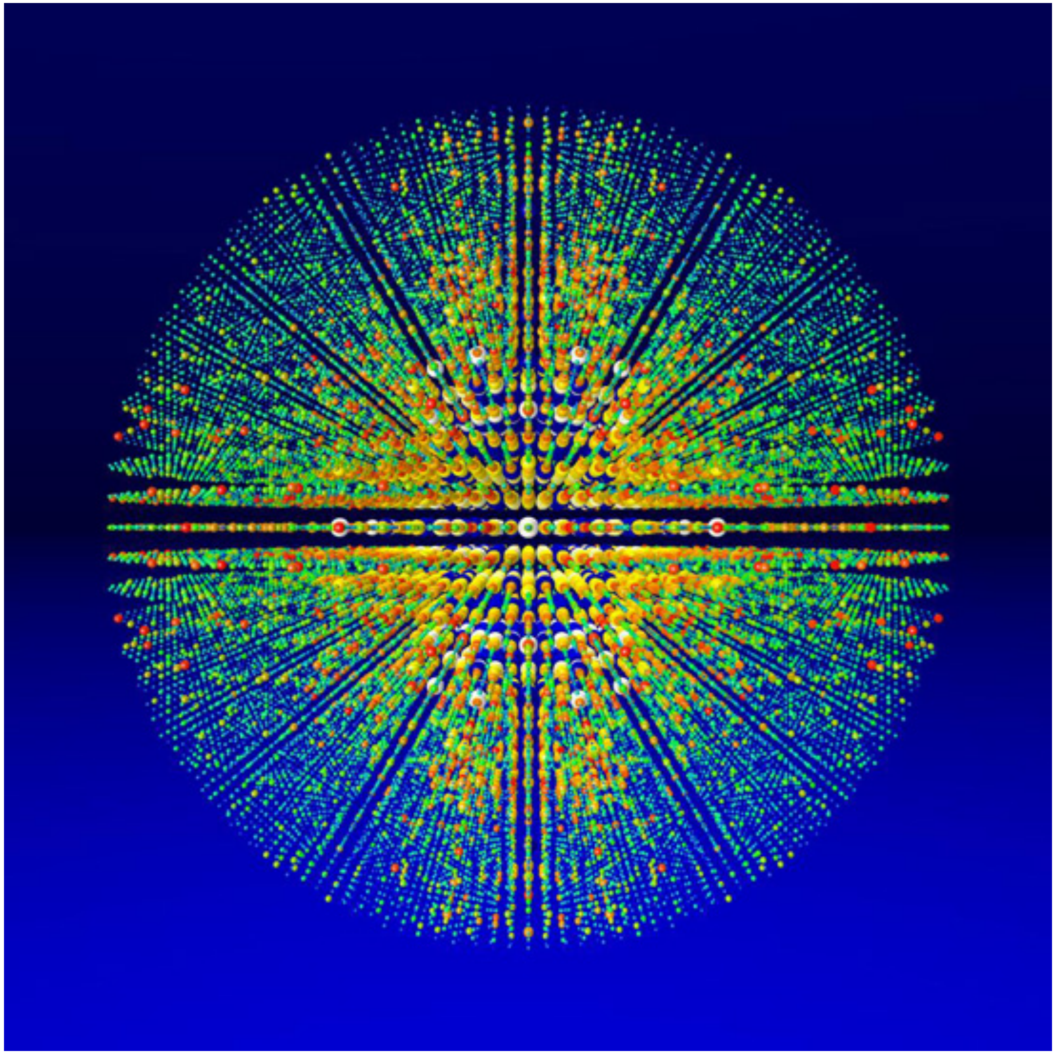

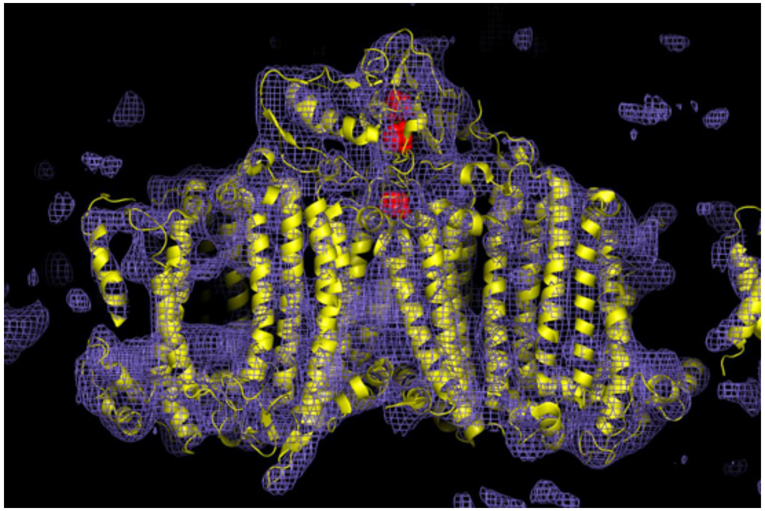

Photosystem I: 3D Visualization of diffraction patterns using serial femtosecond crystallography (left) and electron density map obtained from these diffraction data (top)

Chapman *et al.*, *Nature* **470**, 73 (2011).
Image courtesy: Thomas White, CFEL

High X-ray intensity

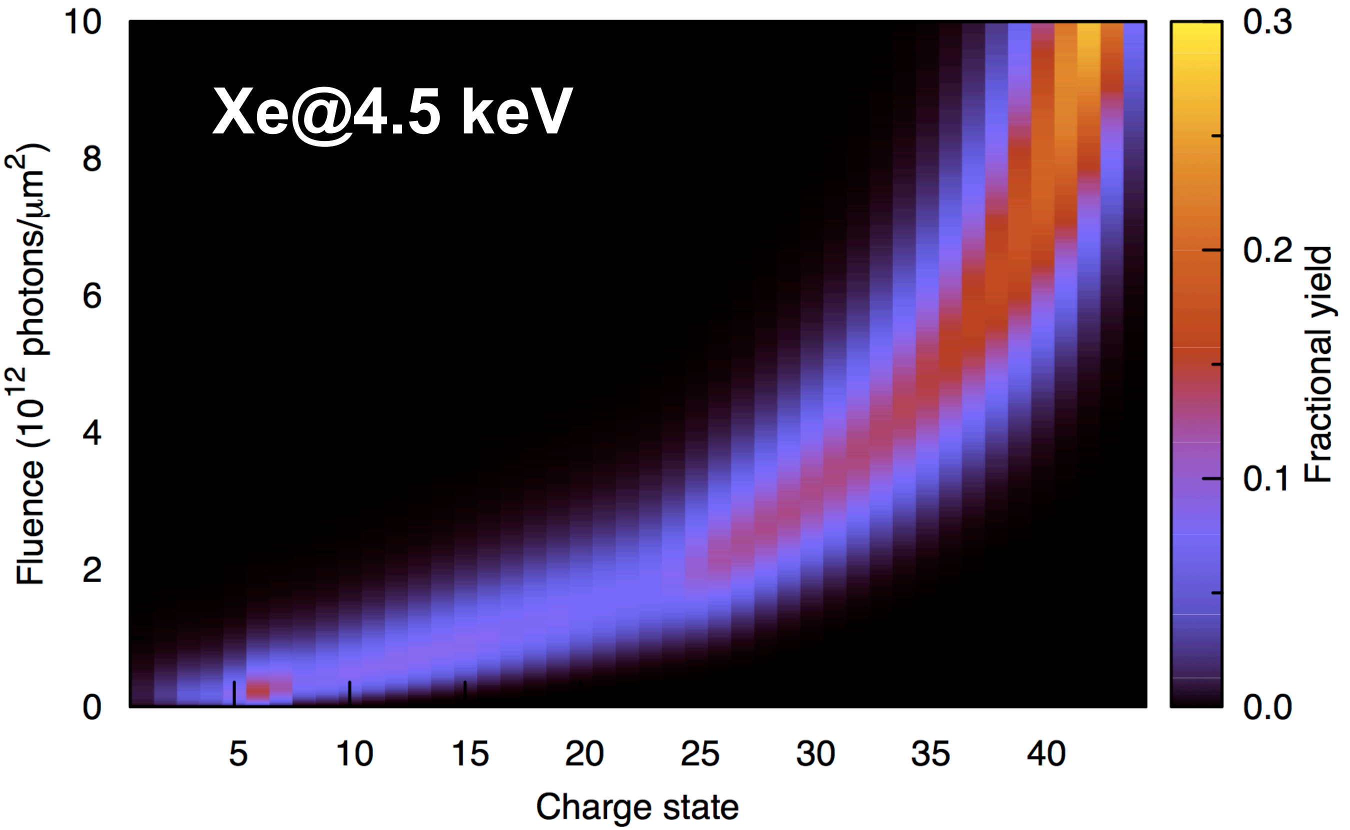

- Here we will discuss only one-photon absorption limit.
- Later you will see more interesting physics with intense x-ray pulses.

Main references

http://xdb.lbl.gov

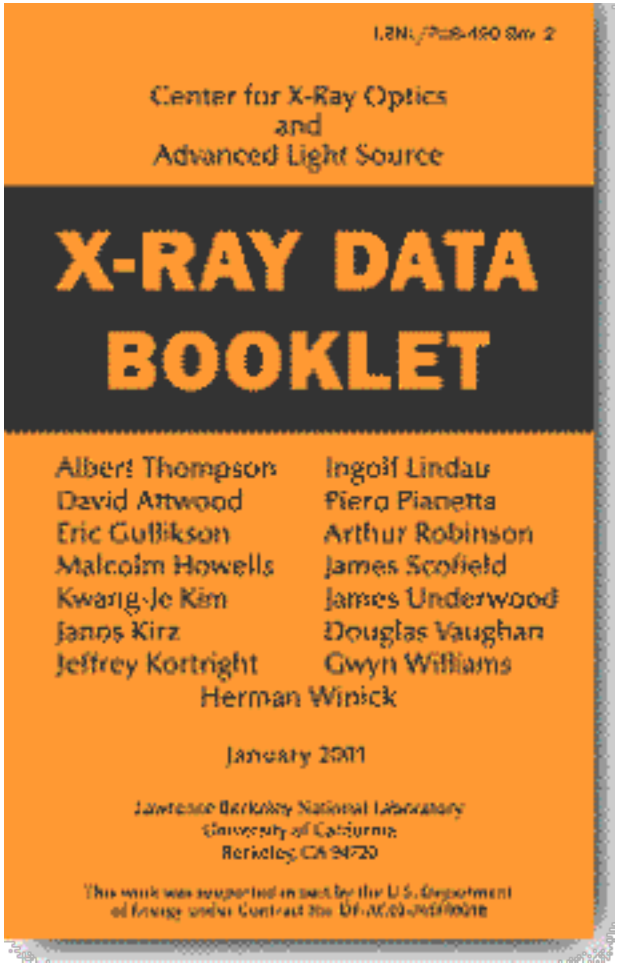

LBNL/PUB-490 Rev. 2

Center for X-Ray Optics
and
Advanced Light Source

X-RAY DATA BOOKLET

Albert Thompson
David Attwood
Eric Gullikson
Malcolm Howells
Kwang-Je Kim
Janos Kirz
Jeffrey Kortright
Ingolf Lindau
Piero Pianetta
Arthur Robinson
James Scofield
James Underwood
Douglas Vaughan
Gwyn Williams
Herman Winick

January 2001

Lawrence Berkeley National Laboratory
University of California
Berkeley, CA 94720

This work was supported in part by the U.S. Department
of Energy under Contract No. [illegible]

R. Santra, *J. Phys. B* **42**, 023001 (2010).

IOP PUBLISHING JOURNAL OF PHYSICS B: ATOMIC, MOLECULAR AND OPTICAL PHYSICS
J. Phys. B: At. Mol. Opt. Phys. **42** (2009) 023001 (16pp) doi:10.1088/0953-4075/42/2/023001

PHD TUTORIAL

Concepts in x-ray physics

Robin Santra

Argonne National Laboratory, Argonne, IL 60439, USA
and
Department of Physics, University of Chicago, Chicago, IL 60637, USA

E-mail: rsantra@anl.gov

Received 26 November 2008
Published 29 December 2008
Online at stacks.iop.org/JPhysB/42/023001

Abstract
A basic introduction to the theory underlying x-ray processes is provided. After general remarks on the practical advantages of using x-rays for probing matter, the derivation of the minimal-coupling Hamiltonian within nonrelativistic quantum electrodynamics is outlined. Perturbation theory is reviewed and applied to describe x-ray-induced processes. In connection with x-ray absorption, inner-shell binding energies and the photon energy dependence of the x-ray absorption cross section are discussed. In the context of x-ray scattering, atomic and molecular scattering factors are introduced, the complex index of refraction is derived, and the nonrelativistic theory of Compton scattering is described. The final topic is x-ray fluorescence and Auger decay of inner-shell-excited systems.

1. Introductory remarks

Since their discovery in the year 1895 by Wilhelm Conrad Röntgen [1], x-rays have become an indispensable tool for studying the structure and electronic properties of matter. Equally important is the role x-rays have come to play in medicine, archaeology, art, security, astronomy and other applications. To date, 19 Nobel prizes have been awarded for x-ray-related research (W C Röntgen 1901, M von Laue 1914, W H Bragg and W L Bragg 1915, C G Barkla 1917, K M G Siegbahn 1924, A H Compton 1927, P J W Debye 1936, H J Muller 1946, M F Perutz and J C Kendrew 1962, F H C Crick, J D Watson, and M H F Wilkins 1962, D Crowfoot Hodgkin 1964, W N Lipscomb 1976, A M Cormack and G N Hounsfield 1979, K M Siegbahn 1981, H A Hauptman and J Karle 1985, J Deisenhofer, R Huber and H Michel 1988, P D Boyer and J E Walker 1997, P Agre and R MacKinnon 2003, R Kornberg 2006).

As a new generation of x-ray sources—so-called x-ray free-electron lasers [2, 3]—is about to come online [4–6], it is timely to familiarize newcomers, experimentalists and theorists alike, with some of the basic properties that make x-rays such a powerful tool. This is attempted in this tutorial. The emphasis is on the development of a consistent theoretical framework that may be employed to describe a variety of x-ray processes. Throughout, the x-rays are assumed to be used as a weak, essentially nonperturbative *probe*. Basic applications of x-rays will be covered. However, since this is a tutorial, there is not a single topic that is discussed in great depth, and some topics, e.g., x-ray sources and x-ray optics [7, 8], are not discussed at all.

This tutorial is structured as follows. In section 2, the derivation of the Hamiltonian underlying nonrelativistic quantum electrodynamics is sketched. This Hamiltonian, in combination with perturbation theory (section 3), allows one to describe all basic x-ray processes. X-ray absorption is the topic of section 4. In section 5, x-ray scattering processes are discussed. Finally, in section 6, relaxation processes following the excitation of an inner-shell electron are treated.

Atomic units are employed, i.e., $m_e = 1, |e| = 1, \hbar = 1$ and $c = 1/\alpha$, where m_e is the electron mass, e is the electron charge, $\hbar$ is Planck's constant divided by $2\pi, c$ is the speed of light in vacuum and $\alpha = \frac{e^2}{\hbar c} \approx 1/137$ is the fine-structure constant. The atomic unit of length is the bohr, $a_0 = \frac{1}{\alpha}\frac{\hbar}{m_e c} \approx 0.529$ Å. The atomic unit of cross section is $a_0^2 \approx 28.0$ Mb, where a *barn* (b) equals 10^{-28} m^2. The atomic unit of energy is the hartree, $E_h = m_e c^2 \alpha^2 \approx 27.2$ eV.

Depending on the photon energy, we typically distinguish between the following two x-ray regimes [7, 8]. Photons with an energy between ~10 E_h (~300 eV) and ~100 E_h (a few keV) are called *soft x-rays*. Soft x-rays cover, roughly, the 1s binding energies for elements ranging from carbon

0953-4075/09/023001+16$30.00 1

How to treat interaction between X-ray and matter?

Total Hamiltonian

$$\hat{H} = \hat{H}_{\mathrm{mol}} + \hat{H}_{\mathrm{EM}} + \hat{H}_{\mathrm{int}}$$

- X-rays interact with the electrons only
- Non-relativistic quantum electrodynamics
- Principle of Minimal Coupling
- Time-dependent perturbation theory

Atomic units used:

$$m_e = 1$$

$$|e| = 1$$

$$\hbar = 1$$

$$1/4\pi\epsilon_0 = 1$$

$$(c = 1/\alpha,\ \ a_0 = 1)$$

Hamiltonian for free electromagnetic field

Hamiltonian for the free electromagnetic field (harmonic oscillator)

$$\hat{H}_{\mathrm{EM}} = \sum_{\boldsymbol{k},\lambda} \omega_{\boldsymbol{k}} \hat{a}^{\dagger}_{\boldsymbol{k},\lambda} \hat{a}_{\boldsymbol{k},\lambda}, \;\; \omega_{\boldsymbol{k}} = |\boldsymbol{k}|/\alpha$$

Field operator: annihilates or creates a photon in the mode (***k***,*λ*).

$$\hat{a}_{\boldsymbol{k},\lambda} |n_{\boldsymbol{k},\lambda}\rangle = \sqrt{n_{\boldsymbol{k},\lambda}} |n_{\boldsymbol{k},\lambda} - 1\rangle$$

$$\hat{a}^{\dagger}_{\boldsymbol{k},\lambda} |n_{\boldsymbol{k},\lambda}\rangle = \sqrt{n_{\boldsymbol{k},\lambda} + 1} |n_{\boldsymbol{k},\lambda} + 1\rangle$$

Commutator relations for photon mode operators

$$[a, b] = ab - ba$$

$$[\hat{a}_{\boldsymbol{k},\lambda}, \hat{a}_{\boldsymbol{k}',\lambda'}] = 0$$

$$[\hat{a}_{\boldsymbol{k},\lambda}, \hat{a}^{\dagger}_{\boldsymbol{k}',\lambda'}] = \delta_{\boldsymbol{k},\boldsymbol{k}'} \delta_{\lambda,\lambda'}$$

$$[\hat{a}^{\dagger}_{\boldsymbol{k},\lambda}, \hat{a}^{\dagger}_{\boldsymbol{k}',\lambda'}] = 0$$

Molecular Hamiltonian

Molecular Hamiltonian

$$\hat{H}_{\mathrm{mol}} = \hat{T}_{\mathrm{N}} + \hat{V}_{\mathrm{NN}} + \hat{H}_{\mathrm{el}}$$

$$\hat{T}_{\mathrm{N}} = -\sum_{a} \frac{\nabla_a^2}{2M_a} \qquad \hat{V}_{\mathrm{NN}} = \sum_{a<a'} \frac{Z_a Z_{a'}}{|\boldsymbol{R}_a - \boldsymbol{R}_{a'}|}$$

Electronic Hamiltonian using the second quantization

$$\hat{H}_{\mathrm{el}} = \int d^3x\, \hat{\psi}^\dagger(\boldsymbol{x}) \left\{ -\frac{\nabla^2}{2} - \sum_a \frac{Z_a}{|\boldsymbol{x} - \boldsymbol{R}_a|} \right\} \hat{\psi}(\boldsymbol{x})$$
$$+ \frac{1}{2} \int d^3x \int d^3x'\, \hat{\psi}^\dagger(\boldsymbol{x}) \hat{\psi}^\dagger(\boldsymbol{x}') \frac{1}{|\boldsymbol{x} - \boldsymbol{x}'|} \hat{\psi}(\boldsymbol{x}') \hat{\psi}(\boldsymbol{x})$$

Anticommutator relations
for electron field operators

$$\{a, b\} = ab + ba$$

$$\{\hat{\psi}_\sigma(\boldsymbol{x}), \hat{\psi}_{\sigma'}(\boldsymbol{x}')\} = 0,$$
$$\{\hat{\psi}_\sigma(\boldsymbol{x}), \hat{\psi}^\dagger_{\sigma'}(\boldsymbol{x}')\} = \delta_{\sigma,\sigma'} \delta^{(3)}(\boldsymbol{x} - \boldsymbol{x}'),$$
$$\{\hat{\psi}^\dagger_\sigma(\boldsymbol{x}), \hat{\psi}^\dagger_{\sigma'}(\boldsymbol{x}')\} = 0.$$

Interaction Hamiltonian

Interaction between electrons and photons
(minimal coupling, Coulomb gauge)

p•A and A²

$$\hat{H}_{\mathrm{int}} = \alpha \int \mathrm{d}^3x \, \hat{\psi}^\dagger(\boldsymbol{x}) \left[\hat{\mathbf{A}}(\boldsymbol{x}) \cdot \frac{\boldsymbol{\nabla}}{\mathrm{i}} \right] \hat{\psi}(\boldsymbol{x}) + \frac{\alpha^2}{2} \int \mathrm{d}^3x \, \hat{\psi}^\dagger(\boldsymbol{x}) \hat{A}^2(\boldsymbol{x}) \hat{\psi}(\boldsymbol{x})$$

Mode expansion of vector potential

$$\hat{\mathbf{A}}(\boldsymbol{x}) = \sum_{\boldsymbol{k},\lambda} \sqrt{\frac{2\pi}{V\omega_{\boldsymbol{k}}\alpha^2}} \left\{ \hat{a}_{\boldsymbol{k},\lambda} \boldsymbol{\epsilon}_{\boldsymbol{k},\lambda} \mathrm{e}^{\mathrm{i}\boldsymbol{k}\cdot\boldsymbol{x}} + \hat{a}^\dagger_{\boldsymbol{k},\lambda} \boldsymbol{\epsilon}^*_{\boldsymbol{k},\lambda} \mathrm{e}^{-\mathrm{i}\boldsymbol{k}\cdot\boldsymbol{x}} \right\}$$

$$\boldsymbol{k} \cdot \boldsymbol{\epsilon}_{\boldsymbol{k},\lambda} = 0, \quad \boldsymbol{\epsilon}^*_{\boldsymbol{k},1} \cdot \boldsymbol{\epsilon}_{\boldsymbol{k},2} = 0$$

p•A: one-photon absorption in first order; one-photon scattering in second order

A²: one-photon scattering in first order

Time-dependent perturbation theory

Full Hamiltonian and unperturbed part $$\hat{H} = \underbrace{\hat{H}_{\mathrm{mol}} + \hat{H}_{\mathrm{EM}}}_{\hat{H}_0} + \hat{H}_{\mathrm{int}}$$

Initial state: $|I\rangle = |\Psi_0^{N_{\mathrm{el}}}\rangle |N_{\mathrm{EM}}\rangle$

Interaction-picture state vector to second order in perturbation

$$\begin{aligned} |\Psi, t\rangle_{\mathrm{int}} = & |I\rangle - \mathrm{i} \int_{-\infty}^{t} \mathrm{d}t' \, \mathrm{e}^{\mathrm{i}\hat{H}_0 t'} \hat{H}_{\mathrm{int}} \mathrm{e}^{-\epsilon|t'|} \mathrm{e}^{-\mathrm{i}\hat{H}_0 t'} |I\rangle \\ & - \int_{-\infty}^{t} \mathrm{d}t' \, \mathrm{e}^{\mathrm{i}\hat{H}_0 t'} \hat{H}_{\mathrm{int}} \mathrm{e}^{-\epsilon|t'|} \mathrm{e}^{-\mathrm{i}\hat{H}_0 t'} \int_{-\infty}^{t'} \mathrm{d}t'' \, \mathrm{e}^{\mathrm{i}\hat{H}_0 t''} \hat{H}_{\mathrm{int}} \mathrm{e}^{-\epsilon|t''|} \mathrm{e}^{-\mathrm{i}\hat{H}_0 t''} |I\rangle + \cdots \end{aligned}$$

Transition rate to second order in perturbation

$$\Gamma_{FI} = 2\pi\delta(E_F - E_I) \left| \langle F|\hat{H}_{\mathrm{int}}|I\rangle + \sum_M \frac{\langle F|\hat{H}_{\mathrm{int}}|M\rangle\langle M|\hat{H}_{\mathrm{int}}|I\rangle}{E_I - E_M - \mathrm{i}\epsilon} + \cdots \right|^2$$

X-ray absorption

X-ray absorption

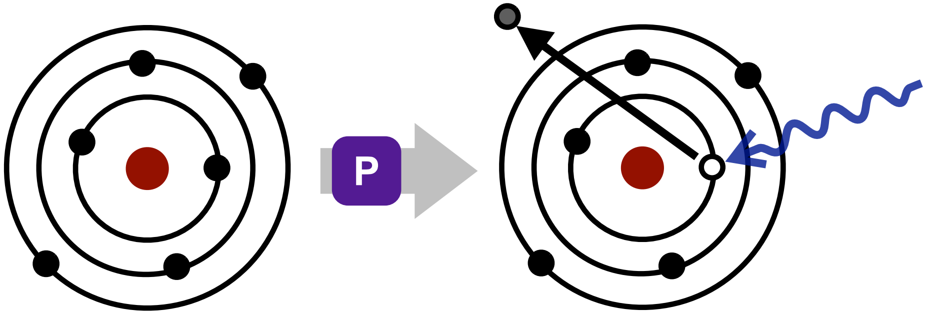

Initial state: $|I\rangle = |\Psi_0^{N_\mathrm{el}}\rangle |N_\mathrm{EM}\rangle$

Final state: $|F\rangle = |\Psi_F^{N_\mathrm{el}}\rangle |N_\mathrm{EM} - 1\rangle$

Absorption rate: $\Gamma_{FI} = 2\pi\delta(E_F - E_I) \left| \langle F | \hat{H}_\mathrm{int} | I \rangle \right|^2$

X-ray absorption cross section

X-ray absorption rate

$$\Gamma_{FI} = \frac{4\pi^2}{\omega_{\text{in}}} \frac{N_{\text{EM}}}{V} \delta\left(E_F^{N_{\text{el}}} - E_0^{N_{\text{el}}} - \omega_{\text{in}}\right)$$
$$\times \left| \langle \Psi_F^{N_{\text{el}}} | \int d^3x \, \hat{\psi}^\dagger(\boldsymbol{x}) e^{i\boldsymbol{k}_{\text{in}}\cdot\boldsymbol{x}} \boldsymbol{\epsilon}_{\boldsymbol{k}_{\text{in}},\lambda_{\text{in}}} \cdot \frac{\boldsymbol{\nabla}}{i} \hat{\psi}(\boldsymbol{x}) | \Psi_0^{N_{\text{el}}} \rangle \right|^2$$

X-ray photon flux

$$J_{\text{EM}} = \frac{1}{\alpha} \frac{N_{\text{EM}}}{V}$$

X-ray absorption cross section

$$\sigma = \Gamma_{FI} / J_{\text{EM}}$$

$$\sigma_F(\boldsymbol{k}_{\text{in}}, \lambda_{\text{in}}) = \frac{4\pi^2}{\omega_{\text{in}}} \alpha \delta\left(E_F^{N_{\text{el}}} - E_0^{N_{\text{el}}} - \omega_{\text{in}}\right)$$
$$\times \left| \underline{\langle \Psi_F^{N_{\text{el}}}} | \int d^3x \, \hat{\psi}^\dagger(\boldsymbol{x}) e^{i\boldsymbol{k}_{\text{in}}\cdot\boldsymbol{x}} \boldsymbol{\epsilon}_{\boldsymbol{k}_{\text{in}},\lambda_{\text{in}}} \cdot \frac{\boldsymbol{\nabla}}{i} \hat{\psi}(\boldsymbol{x}) | \underline{\Psi_0^{N_{\text{el}}} \rangle} \right|^2$$

how to treat many-electron systems?

Electronic many-body problem

Introducing a set of orthonormal spin orbitals $\{\varphi_p(\boldsymbol{x})\}$

which are eigenstates of an one-body Hamiltonian $\hat{F}|\varphi_p\rangle = \varepsilon_p|\varphi_p\rangle$

An electronic one-body Hamiltonian $$\hat{F} = \sum_p \varepsilon_p \hat{c}_p^\dagger \hat{c}_p$$

Creation and annihilation operators for $|\varphi_p\rangle$: $\hat{c}_p^\dagger$ and $\hat{c}_p$

$$\{\hat{c}_p, \hat{c}_q\} = 0,$$
$$\{\hat{c}_p, \hat{c}_q^\dagger\} = \delta_{p,q},$$
$$\{\hat{c}_p^\dagger, \hat{c}_q^\dagger\} = 0.$$

Connecting with the field operators

$$\hat{\psi}(\boldsymbol{x}) = \sum_p \varphi_p(\boldsymbol{x})\hat{c}_p,$$
$$\hat{\psi}^\dagger(\boldsymbol{x}) = \sum_p \varphi_p^\dagger(\boldsymbol{x})\hat{c}_p^\dagger$$

Mean-field model

Independent-electron model $\hat{H}_{\mathrm{el}} \approx \hat{F}$

Mean-field ground state in terms of a single Slater determinant

$$|\Psi_0^{N_{\mathrm{el}}}\rangle \approx |\Phi_0^{N_{\mathrm{el}}}\rangle \equiv \prod_{i=1}^{N_{\mathrm{el}}} \hat{c}_i^\dagger |\mathrm{vacuum}\rangle$$

Mean-field ground-state energy $E_0^{N_{\mathrm{el}}} \approx \langle \Phi_0^{N_{\mathrm{el}}} | \hat{F} | \Phi_0^{N_{\mathrm{el}}} \rangle = \sum_{i=1}^{N_{\mathrm{el}}} \varepsilon_i$

Hartree-Fock (HF) method: minimizing $\langle \Phi_0^{N_{\mathrm{el}}} | \hat{H}_{\mathrm{el}} | \Phi_0^{N_{\mathrm{el}}} \rangle$

the best choice among the mean-field models

Koopmans' theorem

One-hole state
$$|\Phi_i^{N_\mathrm{el}-1}\rangle \equiv \hat{c}_i |\Phi_0^{N_\mathrm{el}}\rangle$$

Energy of one-hole state
$$E_i^{N_\mathrm{el}-1} \approx \langle\Phi_i^{N_\mathrm{el}-1}|\hat{F}|\Phi_i^{N_\mathrm{el}-1}\rangle = \left\{\sum_{j=1}^{N_\mathrm{el}} \varepsilon_j\right\} - \varepsilon_i$$

Ionization potential
$$I_i \equiv E_i^{N_\mathrm{el}-1} - E_0^{N_\mathrm{el}} \approx -\varepsilon_i$$

Koopmans' theorem: valid for HF orbitals

$$\begin{aligned} I_i =& \langle\Phi_i^{N_\mathrm{el}-1}|\hat{H}_\mathrm{el}|\Phi_i^{N_\mathrm{el}-1}\rangle \\ &- \langle\Phi_0^{N_\mathrm{el}}|\hat{H}_\mathrm{el}|\Phi_0^{N_\mathrm{el}}\rangle = -\varepsilon_i \end{aligned}$$

Note: Koopmans received a Nobel prize in Economics in 1975, of course, not for this theorem.

For Neon,

Koopmans	EXP
$-\varepsilon_{2p} = 23.1$ eV	21.6 eV
$-\varepsilon_{2s} = 52.5$ eV	48.5 eV
$-\varepsilon_{1s} = 892$ eV	870 eV

X-ray absorption within mean-field model

Particle-hole state $|\Phi_i^a\rangle \equiv \hat{c}_a^\dagger |\Phi_i^{N_{\mathrm{el}}-1}\rangle = \hat{c}_a^\dagger \hat{c}_i |\Phi_0^{N_{\mathrm{el}}}\rangle$

Initial state $|I\rangle = |\Phi_0^{N_{\mathrm{el}}}\rangle |N_{\mathrm{EM}}\rangle$

Final state $|F\rangle = \hat{c}_a^\dagger \hat{c}_i |\Phi_0^{N_{\mathrm{el}}}\rangle |N_{\mathrm{EM}}-1\rangle$

Cross section for particle-hole transition

$$\sigma_i^a(\boldsymbol{k}_{\mathrm{in}}, \lambda_{\mathrm{in}}) = \frac{4\pi^2}{\omega_{\mathrm{in}}} \alpha \delta(\varepsilon_a + I_i - \omega_{\mathrm{in}}) \left| \langle \varphi_a | \mathrm{e}^{\mathrm{i}\boldsymbol{k}_{\mathrm{in}} \cdot \boldsymbol{x}} \boldsymbol{\epsilon}_{\boldsymbol{k}_{\mathrm{in}}, \lambda_{\mathrm{in}}} \cdot \frac{\boldsymbol{\nabla}}{\mathrm{i}} | \varphi_i \rangle \right|^2$$

Energy of excited electron $\varepsilon_a = \omega_{\mathrm{in}} - I_i > 0$ **"Photoelectric effect"**

Note: Einstein received a Nobel prize in 1921 for the photoelectric effect, not for theory of relativity.

Subshell x-ray absorption cross section

$$\sigma_i(\boldsymbol{k}_{\mathrm{in}}, \lambda_{\mathrm{in}}) = \sum_a \sigma_i^a(\boldsymbol{k}_{\mathrm{in}}, \lambda_{\mathrm{in}})$$

CFEL SCIENCE

DESY.

K-shell photoionization: a simple model

- After employing the dipole approximation and atomic orbitals

$$\sigma_P(i,\omega) = \frac{4}{3}\alpha\pi^2\omega N_i \sum_{l_j=|l_i-1|}^{l_i+1} \frac{l_>}{2l_i+1} \left| \int_0^\infty u_{n_i l_i}(r) u_{\varepsilon l_j}(r) r dr \right|^2$$

- Simple model of an atomic species of atomic number *Z*
  - 1*s* orbital ~ H-like 1*s* orbital of *Z*, $u_{1s}(r) \sim Z^{3/2} r e^{-Zr}$, $I_{1s} = Z^2/2$
  - photoelectron wave function ~ plane wave (assuming $\omega_\text{in} \gg I_{1s}$)
- At fixed photon energy *ω*, $\sigma_P \sim Z^5$

  Compare σ_C (*Z*=6) and σ_Ca (*Z*=20): $(20/6)^5$ ~ 400 times

- At fixed *Z*, $\sigma_P \sim \omega_\text{in}^{-7/2}$

  For a given atom, the x-ray absorption cross section above the 1*s* threshold decreases with increasing photon energy.

Photoionization cross section calculation

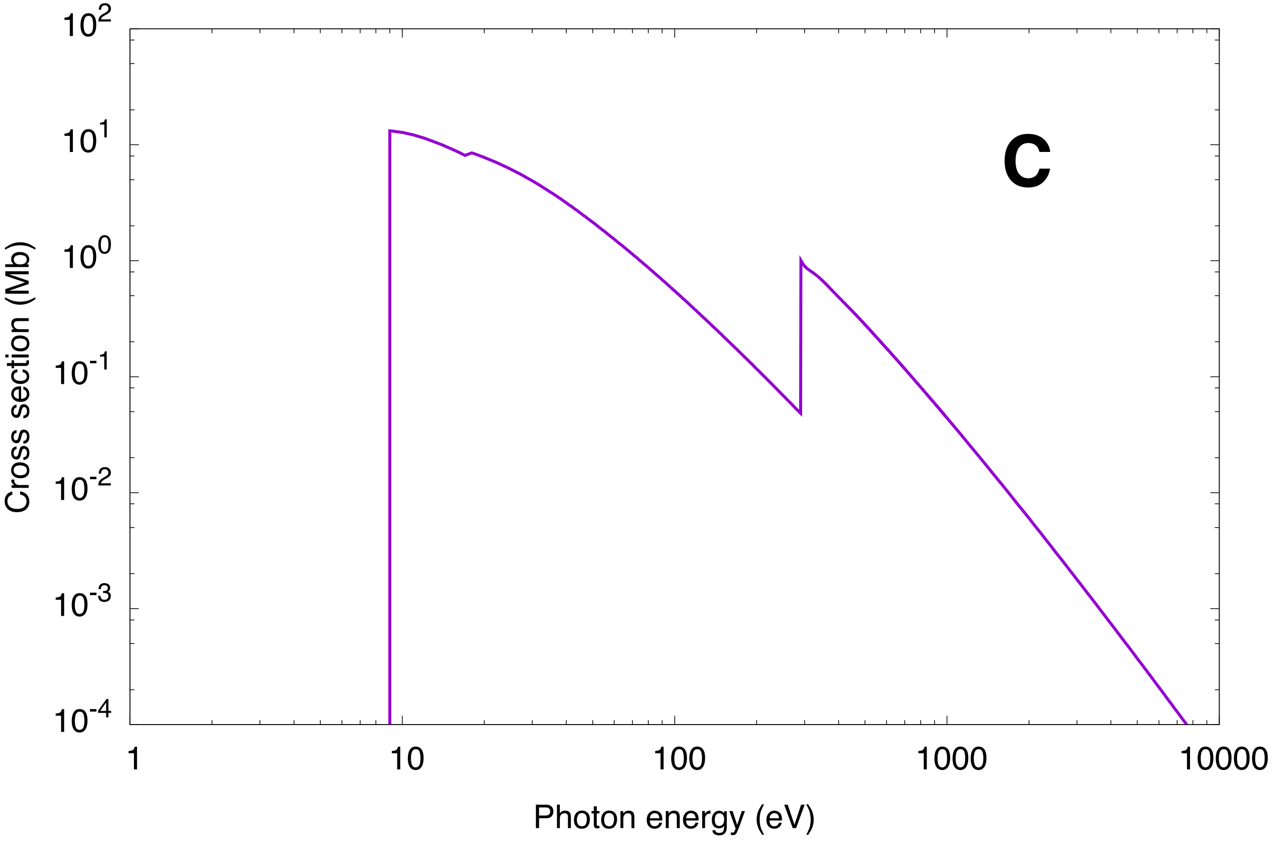

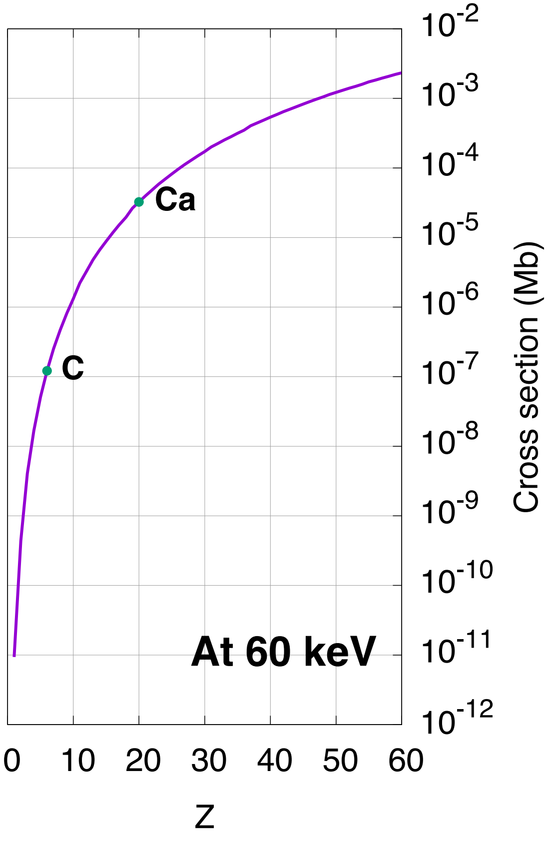

- PCS changes by varying ω and Z; edge structures

Table of photoionization cross sections

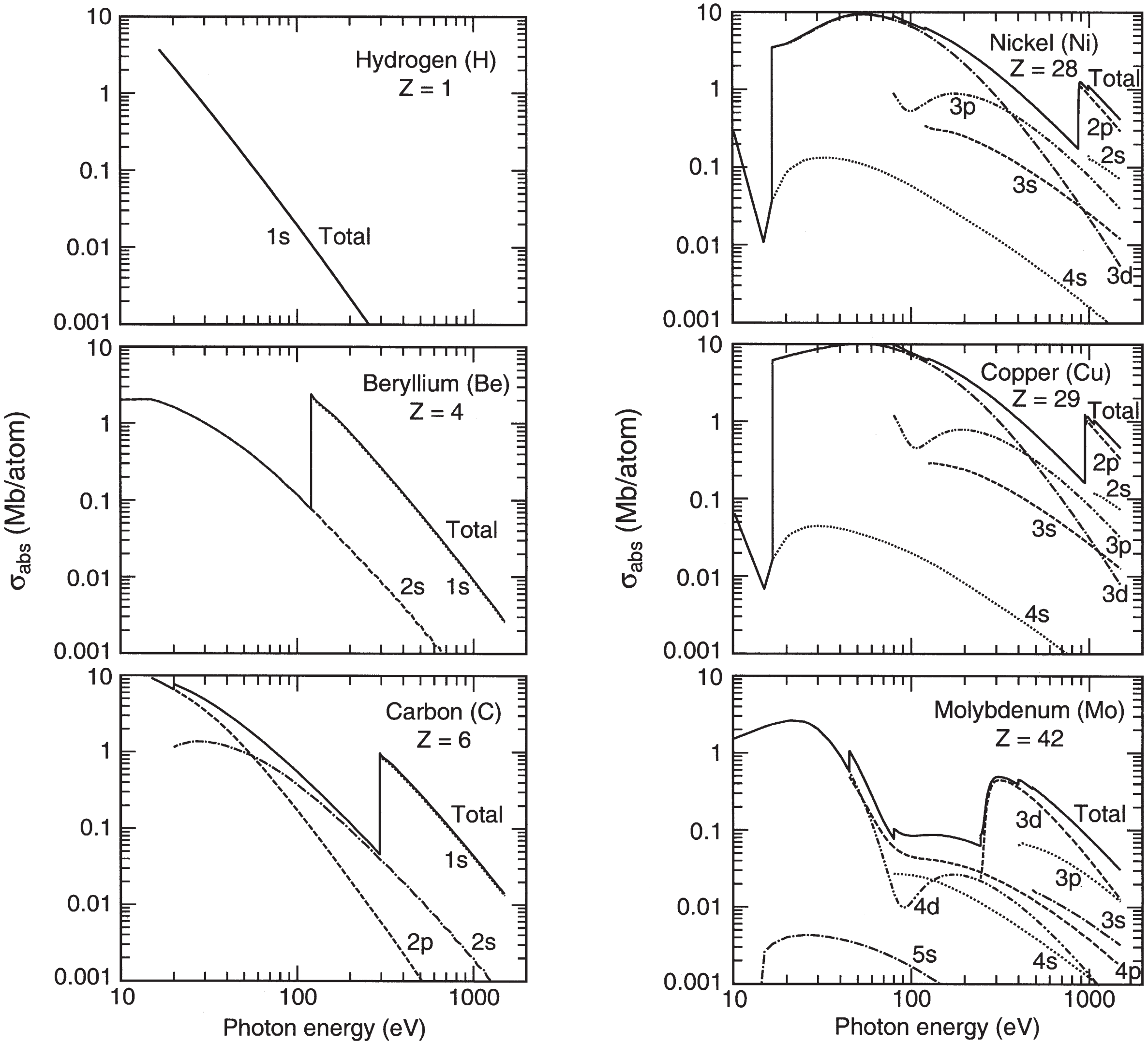

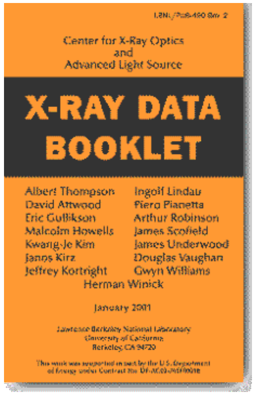

Center for X-Ray Optics
and
Advanced Light Source

X-RAY DATA BOOKLET

Albert Thompson
David Attwood
Eric Gullikson
Malcolm Howells
Kwang-Je Kim
Janos Kirz
Jeffrey Kortright
Ingolf Lindau
Piero Pianetta
Arthur Robinson
James Scofield
James Underwood
Douglas Vaughan
Gwyn Williams
Herman Winick

January 2001

Lawrence Berkeley National Laboratory
University of California
Berkeley, CA 94720

or

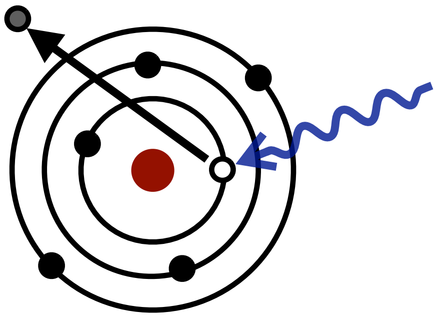

running XATOM

Applications of X-ray absorption

- X-ray photoelectron spectroscopy (XPS): measuring *photoelectron energy*
  - PES: Photo-Electron Spectroscopy or Photo-Emission Spectroscopy
  - ESCA: Electron Spectroscopy for Chemical Analysis
- X-ray absorption spectroscopy (XAS): measuring *absorption cross section* as a function of *photon energy*
  - XANES: X-ray Absorption Near-Edge Structure
    NEXAFS: Near Edge X-Ray Absorption Fine Structure
  - EXAFS: Extended X-ray Absorption Fine Structure

XPS: X-ray Photoelectron Spectroscopy

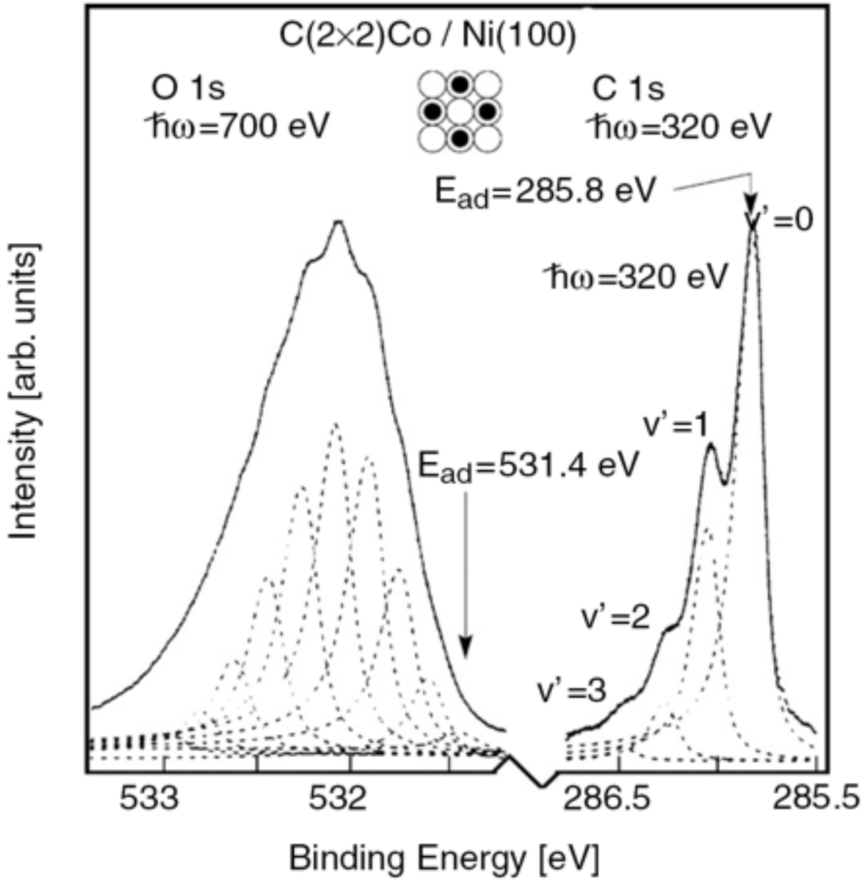

Figure 8. High-resolution XPS spectra of C1s and O1s from a $c(2\times2)$ CO/Ni(1 0 0) [38]. The fine structure is due to intramolecular stretch vibrations of the adsorbed CO molecules.

PES: Photo-Emission
(or Photo-Electron)
Spectroscopy

$$\underset{\text{measured}}{\underset{\uparrow}{\varepsilon_a}} = \underset{\text{fixed}}{\underset{\uparrow}{\omega_{\text{in}}}} - I_i$$

ESCA: Electron Spectroscopy for Chemical Analysis

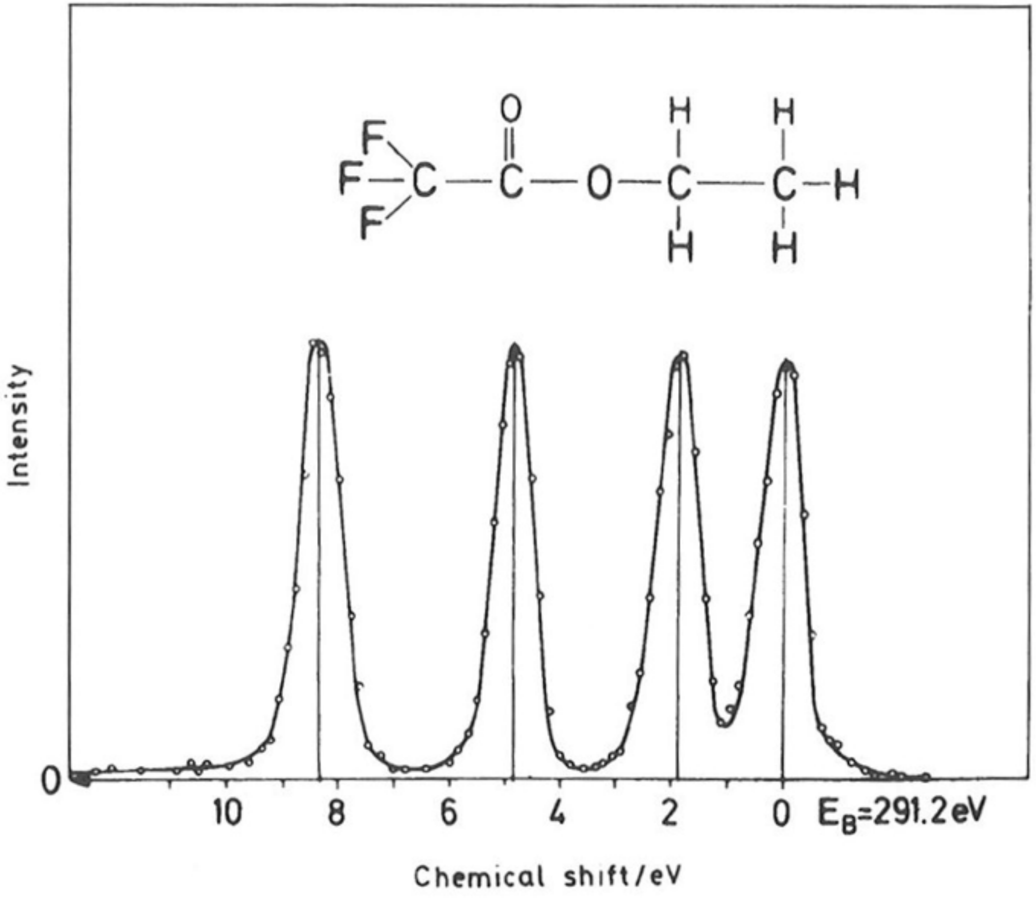

Figure 8.14 The monochromatized Al*K*α carbon 1*s* XPS spectrum of ethyltrifluoroacetate showing the chemical shifts relative to an ionization energy of 291.2 eV. (Reproduced, with permission, from Gelius, U., Basilier, E., Svensson, S., Bergmark, T., and Siegbahn, K., *J. Electron Spectrosc.*, **2**, 405, 1974)

$$\underset{\text{measured}}{\underset{\uparrow}{\varepsilon_a}} = \underset{\text{fixed}}{\underset{\uparrow}{\omega_{\text{in}}}} - I_i$$

ESCA molecule:
first molecule used for ESCA by Kai Siegbahn (Nobel prize in 1981)

XAS: X-ray Absorption Spectroscopy

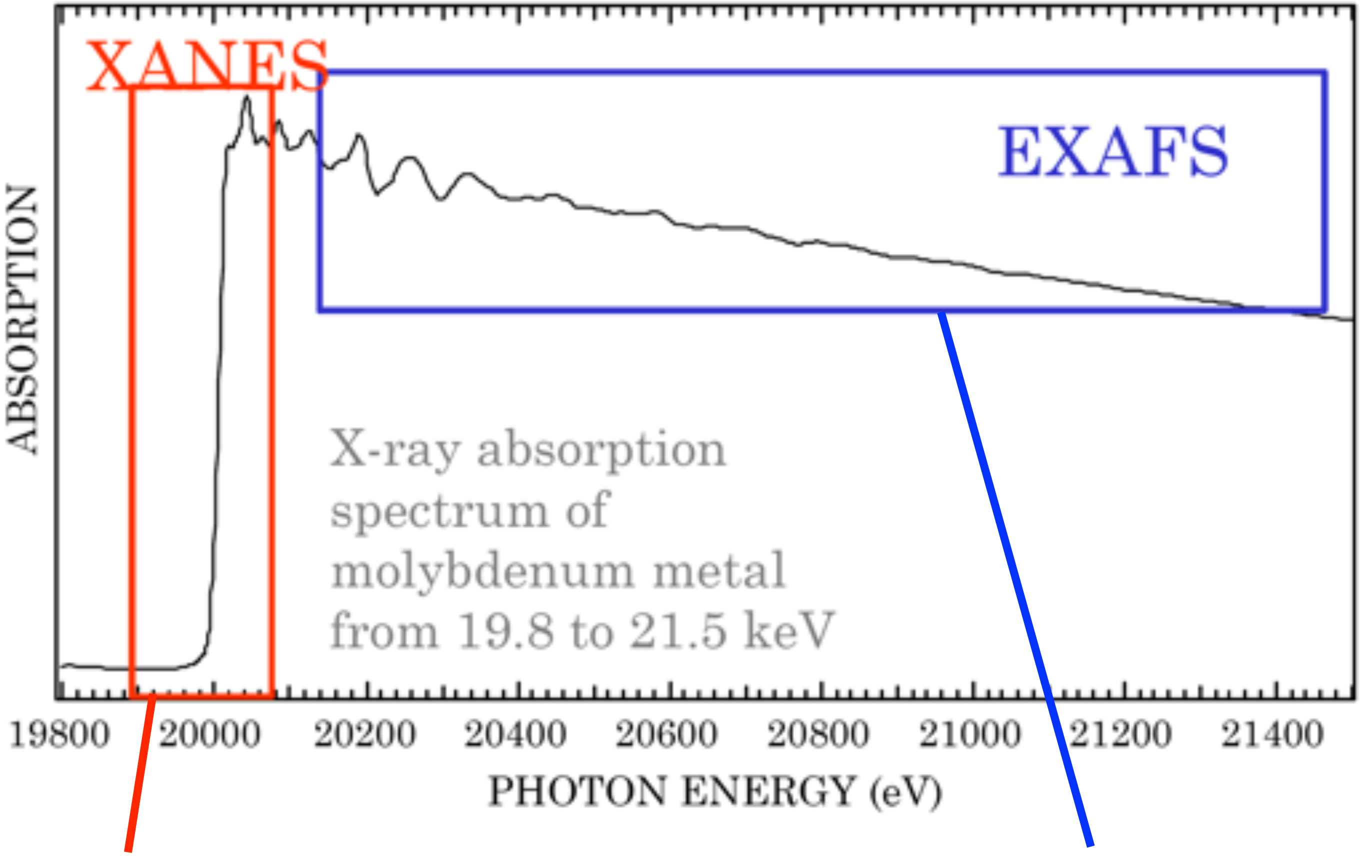

$$\varepsilon_a = \omega_{\text{in}} - I_i$$

↑

varied

solid target:
transmission

gas phase or very
dilute target:
fluorescence

NE: depends on local coordination environment and oxidation state

E: depends on nearest-neighbor geometry

EXAFS: Extended X-ray Absorption Fine Structure

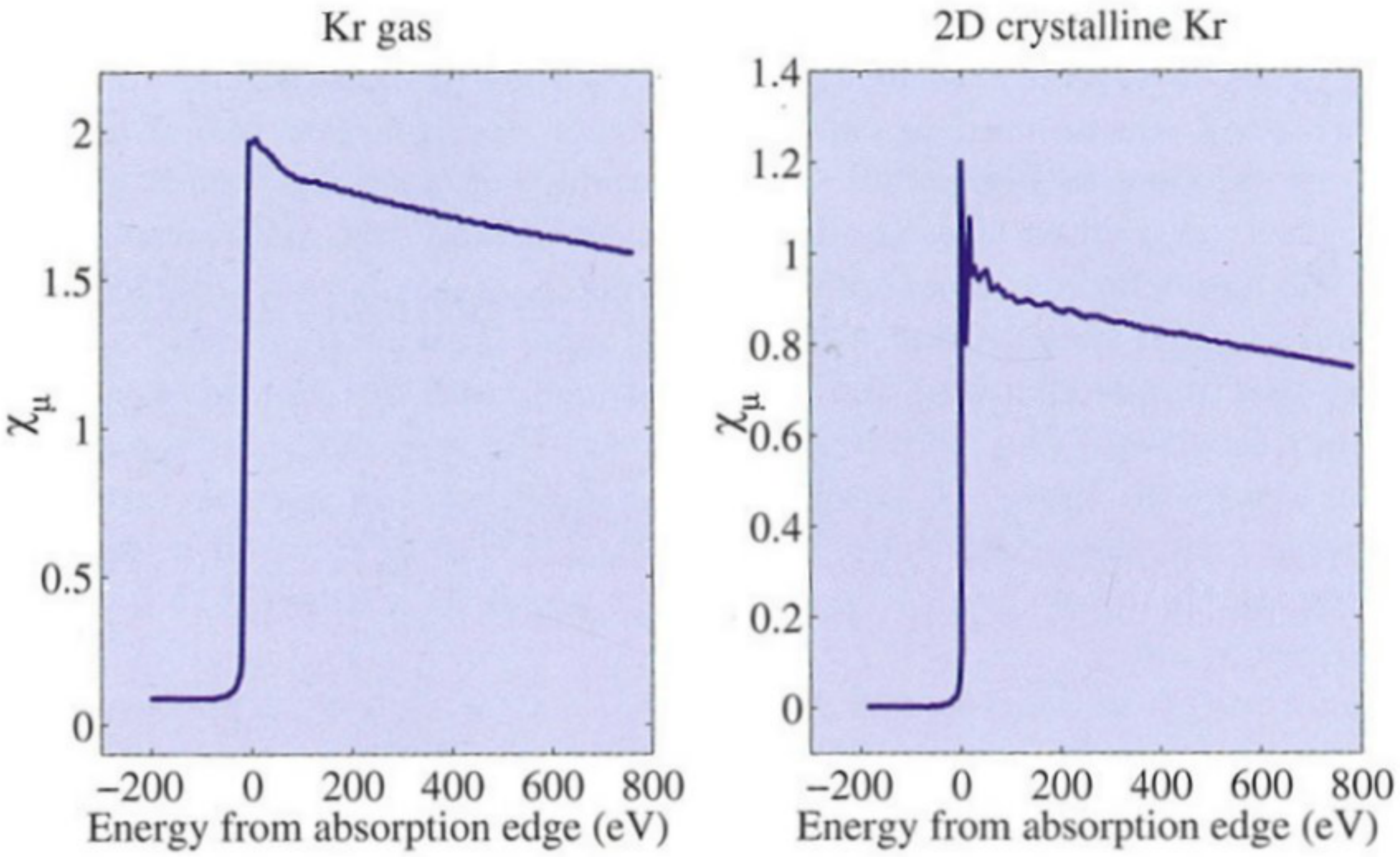

EXAFS reflects nearest-neighbor geometry and
it is highly sensitive to changes in bond lengths.

XANES: X-ray Absorption Near-Edge Structure

Also called **NEXAFS**: Near-Edge X-ray Absorption Fine Structure

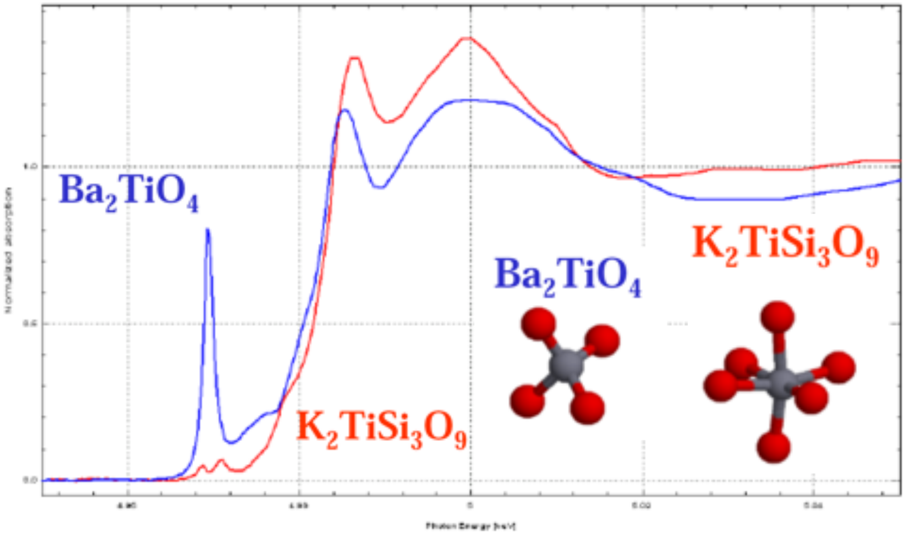

different coordination environments

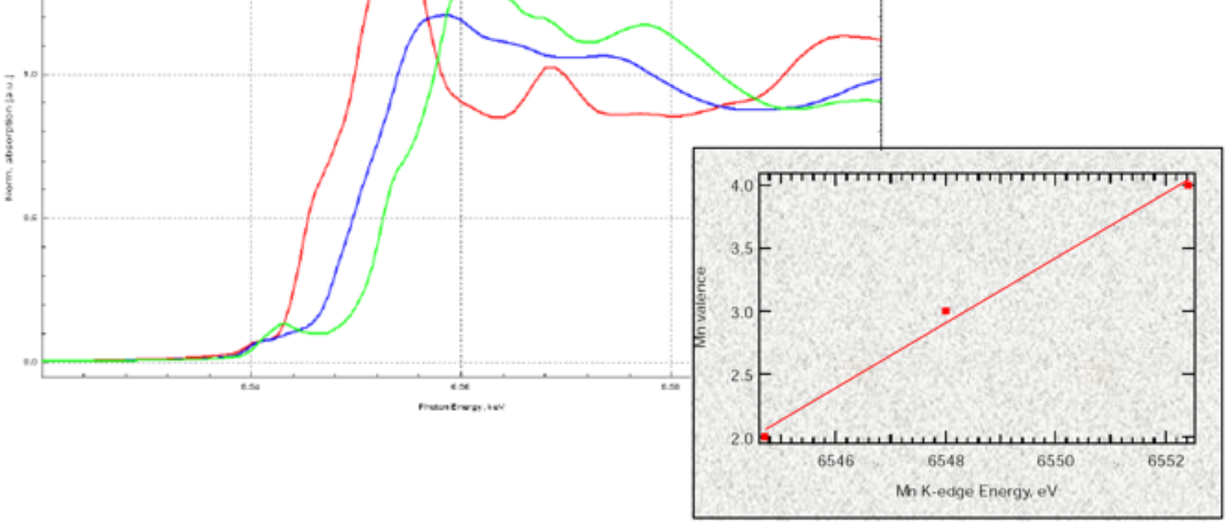

different oxidation states

Summary

- X-rays can probe atomic structure and electronic structure of matter.
- X-rays interact with the electrons only.
- Hamiltonians for EM, molecule, and interaction between them

$$\hat{H} = \hat{H}_{\mathrm{mol}} + \hat{H}_{\mathrm{EM}} + \hat{H}_{\mathrm{int}}$$

- The mean-field theory for electronic many-body problem
- Transition rate calculated within the time-dependent perturbation theory

$$\Gamma_{FI} = 2\pi\delta(E_F - E_I)\left|\langle F|\hat{H}_{\mathrm{int}}|I\rangle\right|^2$$

- The theoretical framework applied for calculating a photoabsorption cross section
- X-ray absorption applications: XPS, ESCA, XAS, XANES, EXAFS, …

X-ray atomic physics on computer:
XATOM

XATOM: all about x-ray atomic physics

- Computer program suite to describe dynamical behaviors of atoms interacting with XFEL pulses
- Uses the Hartree-Fock-Slater model
- Calculates all cross sections and rates of x-ray-induced processes for any given element

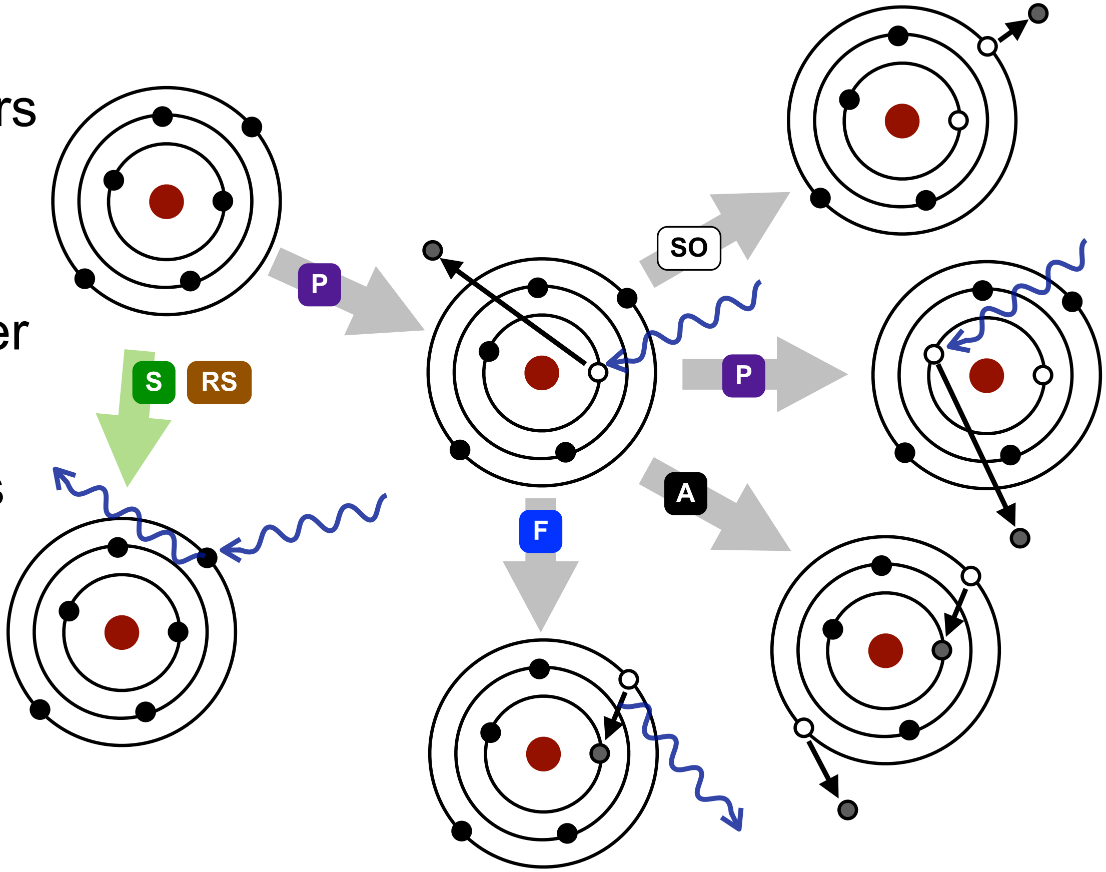

Son, Young & Santra,
Phys. Rev. A **83**, 033402 (2011).

Jurek, Son, Ziaja & Santra,
J. Appl. Cryst. **49**, 1048–1056 (2016).

https://www.desy.de/~xraypac/

Dynamical behavior of atom in XFEL pulses

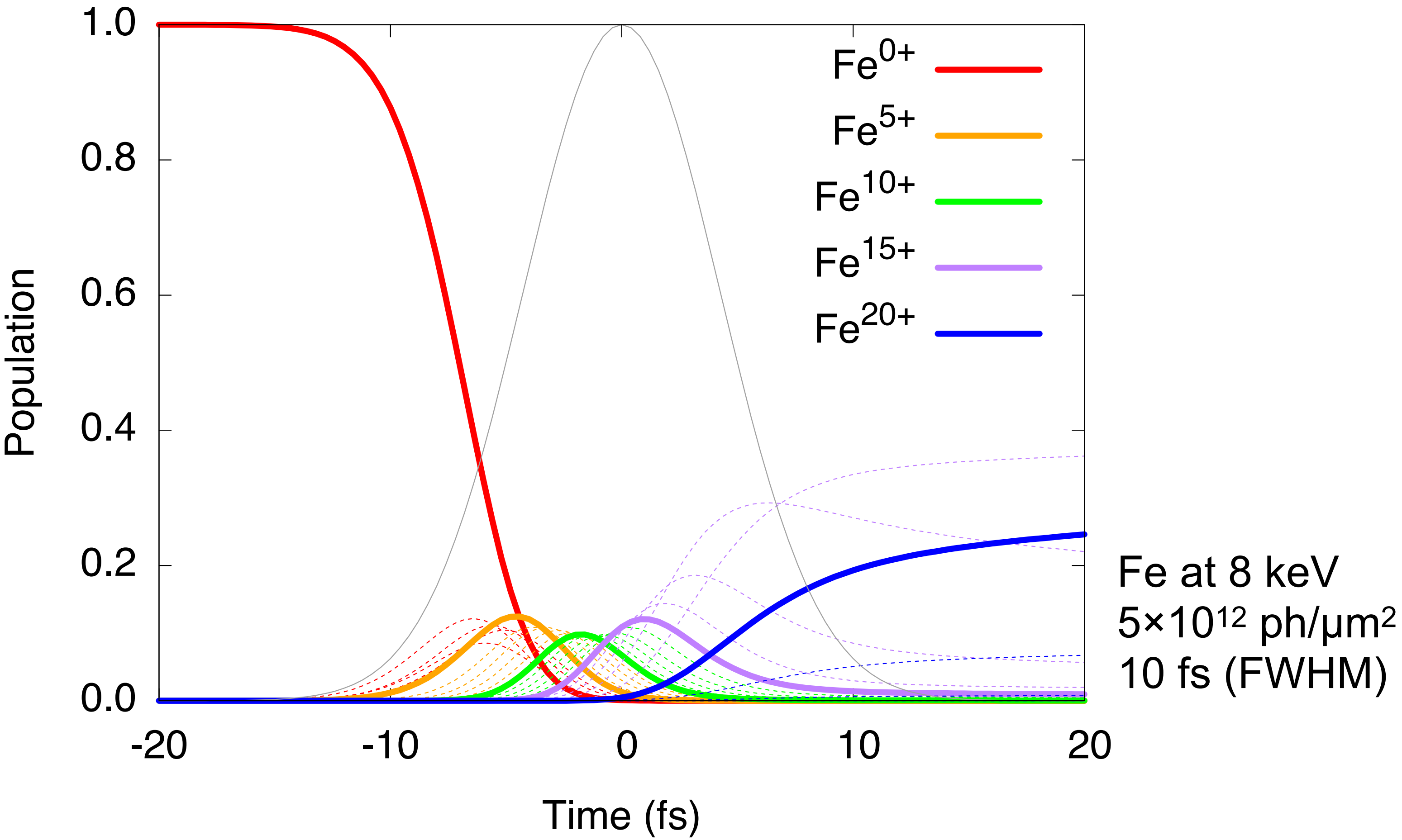

Son, Chapman & Santra, *Phys. Rev. Lett.* **107**, 218102 (2011).

Photoionization cross section calculation

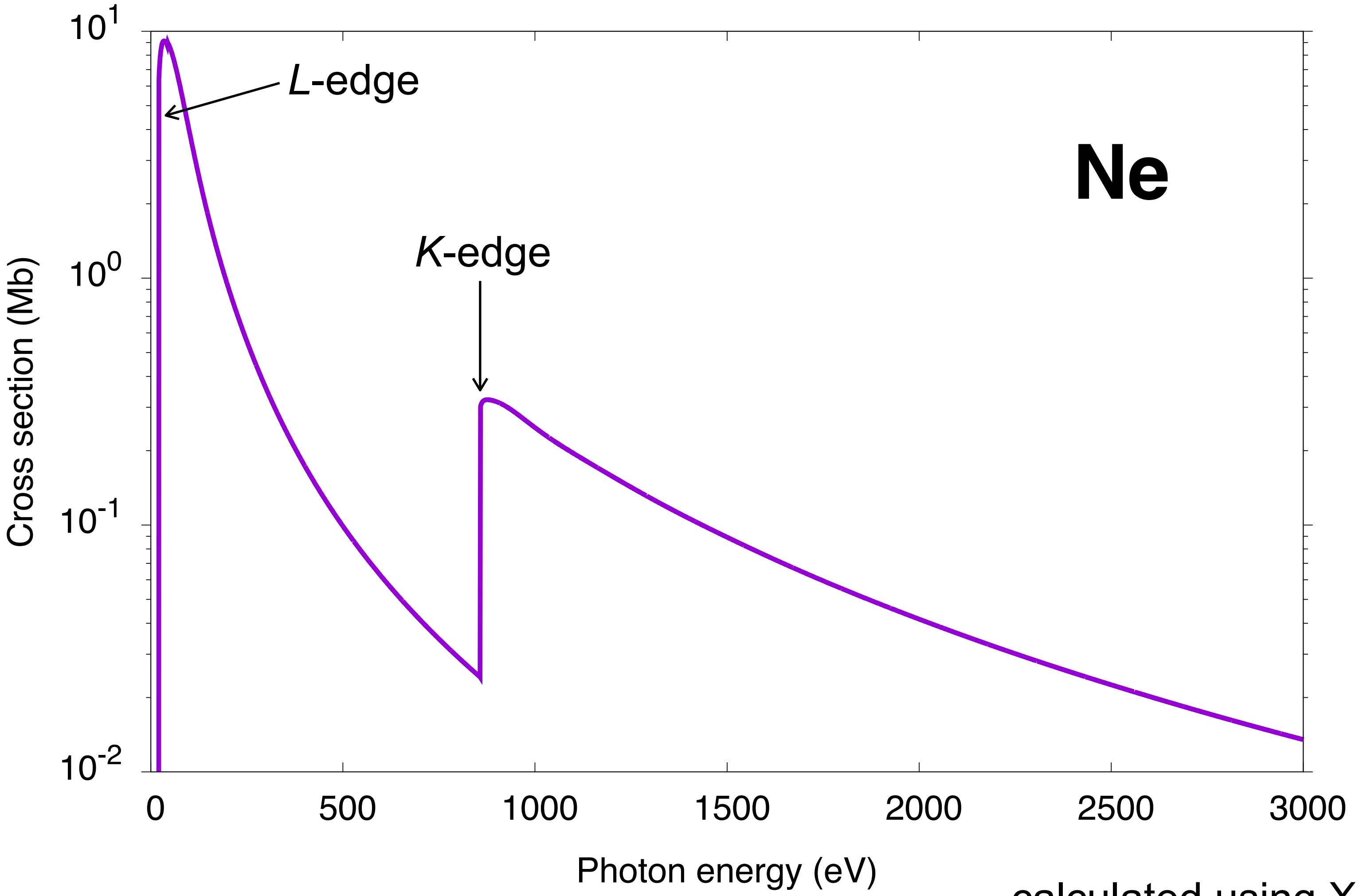

calculated using XATOM

Outline

- First day (August 2, 2021)
  - Introduction
  - Theory of X-ray–matter interaction
  - X-ray absorption
  - X-ray atomic physics on computer: XATOM
- Second day (August 3, 2021)
  - X-ray fluorescence
  - Auger-Meitner decay
  - X-ray scattering
  - Computer simulations with XATOM

Relaxation processes

Decay of inner-shell-excited systems

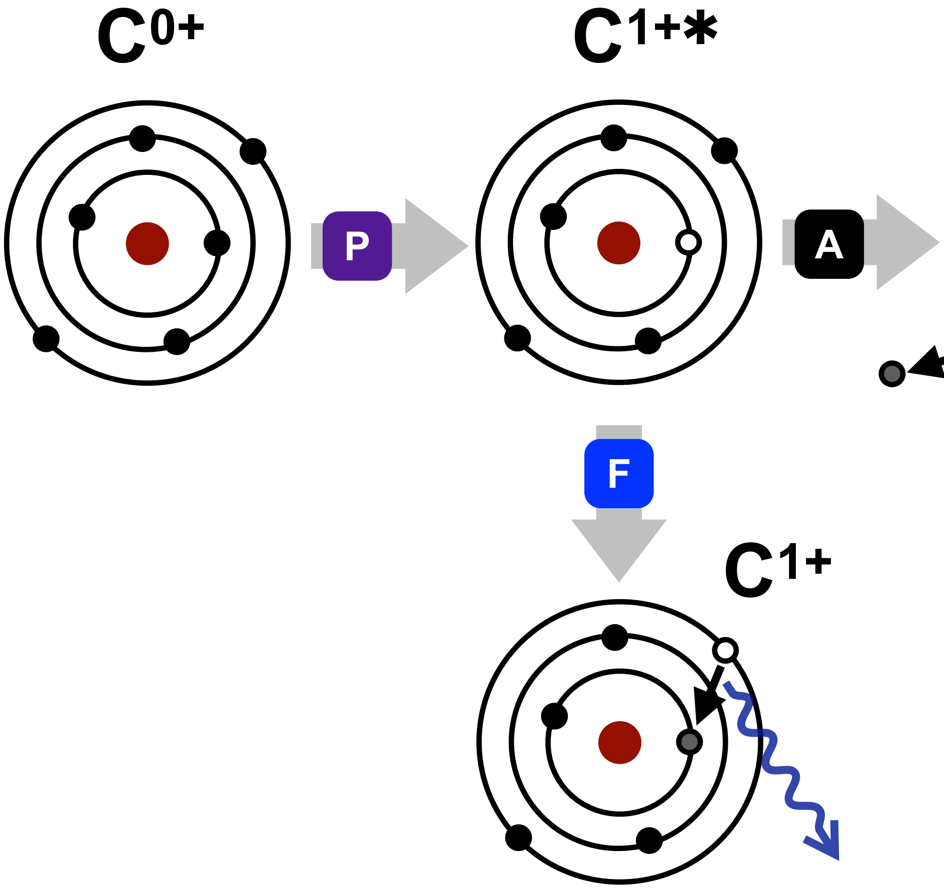

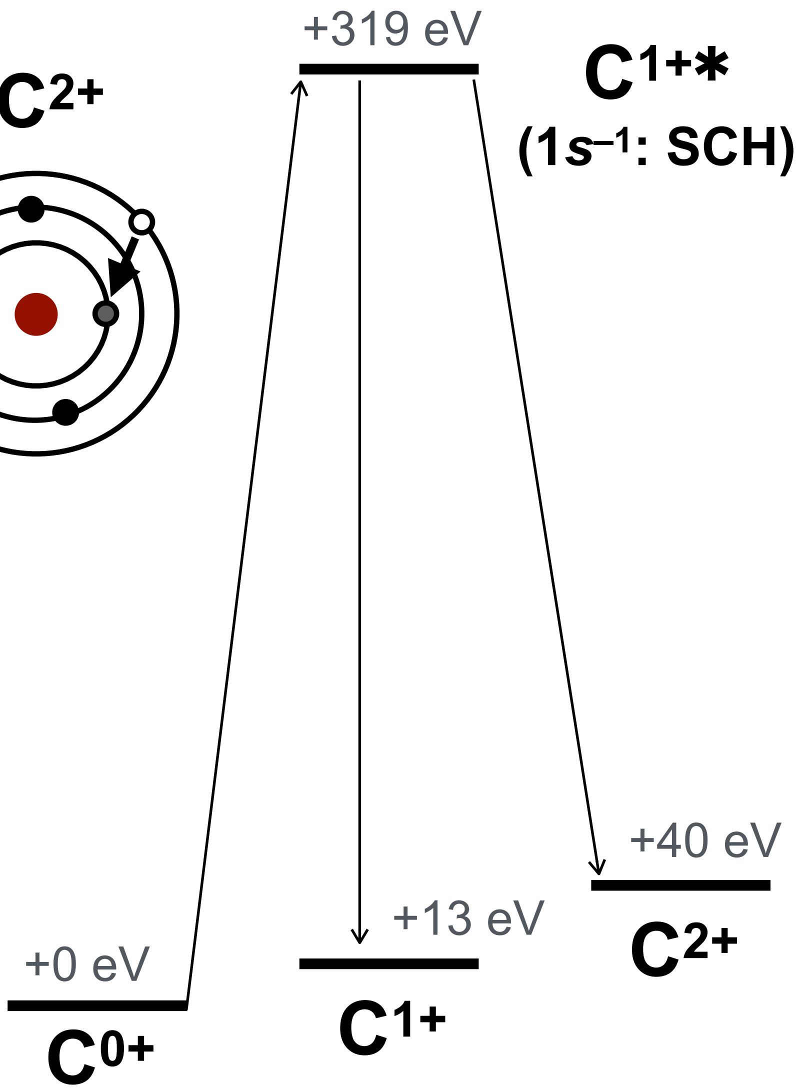

X-ray fluorescence within mean-field model

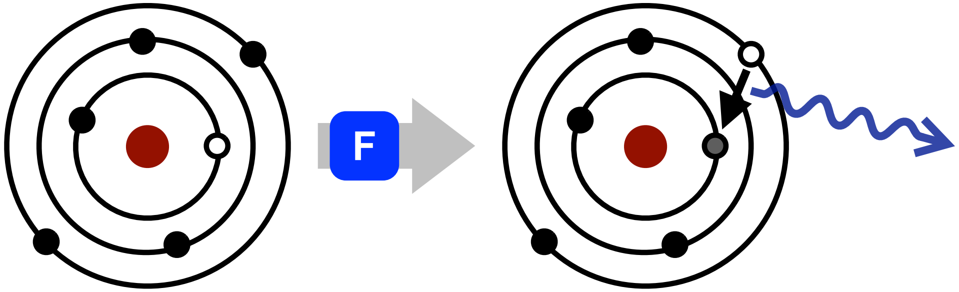

Initial state: $$|I\rangle = \hat{c}_i |\Phi_0^{N_\mathrm{el}}\rangle |0\rangle$$

Final state: $$|F\rangle = \hat{c}_{i'} |\Phi_0^{N_\mathrm{el}}\rangle \hat{a}^\dagger_{\boldsymbol{k}_F,\lambda_F} |0\rangle$$

Fluorescence rate: $$\Gamma_{FI} = 2\pi\delta(E_F - E_I) \left| \langle F | \hat{H}_\mathrm{int} | I \rangle \right|^2$$

X-ray fluorescence rate and energy

Partial X-ray fluorescence rate

$$\Gamma_{FI} = 2\pi\delta\left(E_F - E_I\right)\left|\langle F|\hat{H}_{\text{int}}|I\rangle\right|^2$$

$$= \frac{4\pi^2}{V\omega_F}\delta(I_{i'} + \omega_F - I_i)\left|\langle\varphi_i|e^{-\mathrm{i}\boldsymbol{k}_F\cdot\boldsymbol{x}}\boldsymbol{\epsilon}^*_{\boldsymbol{k}_F,\lambda_F}\cdot\frac{\nabla}{\mathrm{i}}|\varphi_{i'}\rangle\right|^2$$

$$\Gamma_{i,i'} = \sum_{\boldsymbol{k}_F,\lambda_F}\Gamma_{FI} = \sum_{\lambda_F}\frac{V}{(2\pi)^3}\int\mathrm{d}\Omega_F\int_0^\infty \mathrm{d}k_F\, k_F^2\Gamma_{FI}$$

X-ray fluorescence energy $\omega_F = I_i - I_{i'}$

X-ray fluorescence transition lines

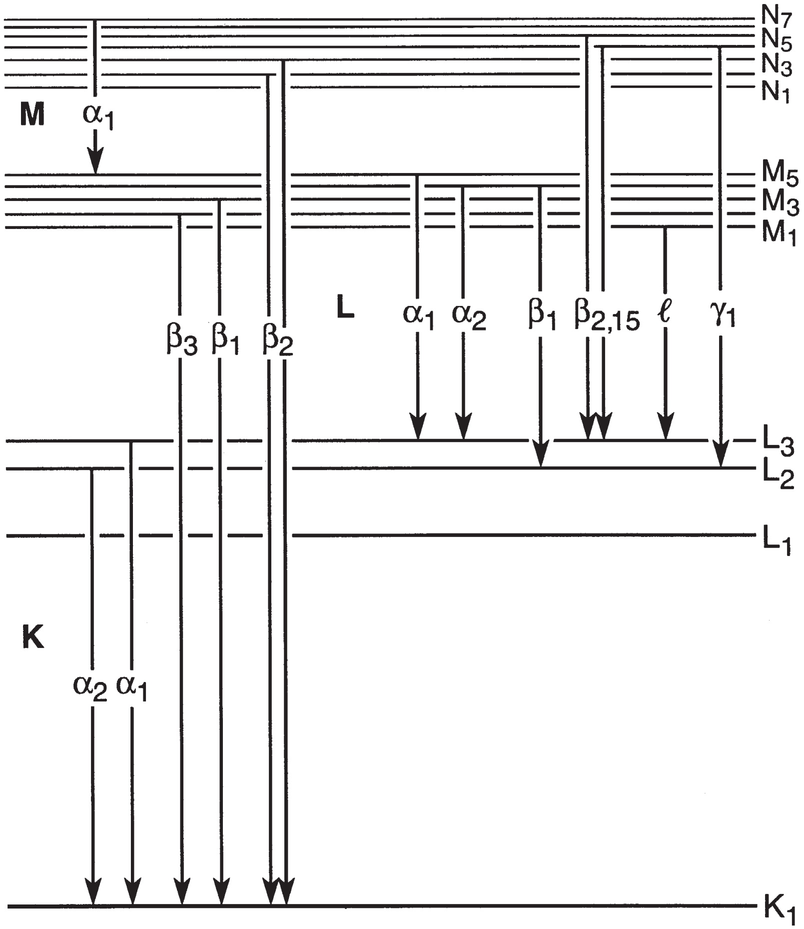

Fig. 1-1. *Transitions that give rise to the emission lines in Table 1-3.*

Characteristic transition energies
➔ fingerprint of elements

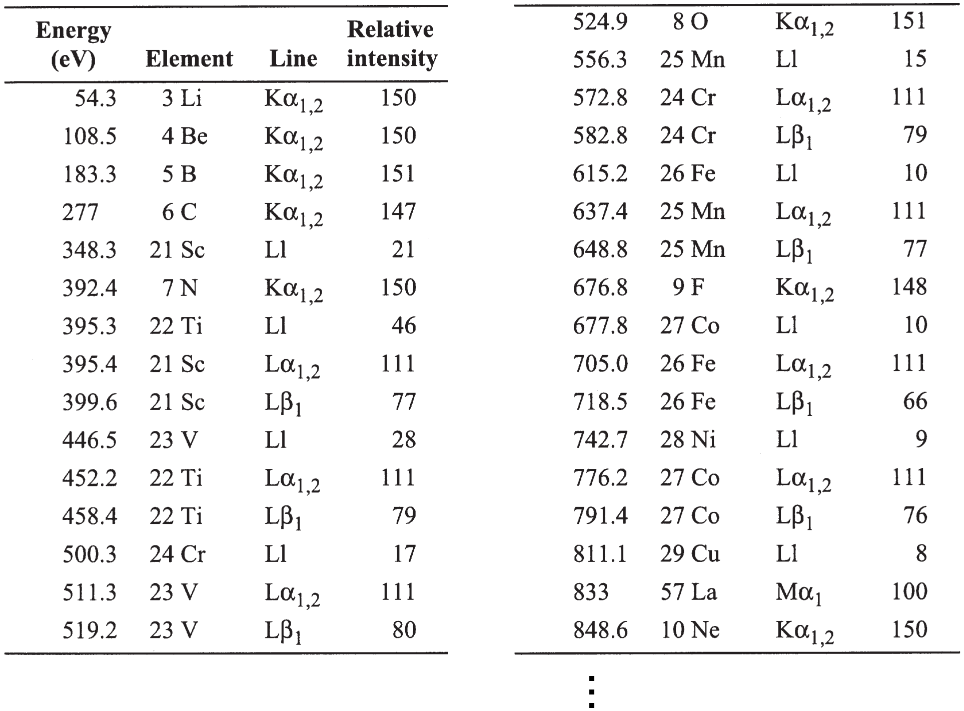

Energy (eV)	Element	Line	Relative intensity
54.3	3 Li	K$\alpha_{1,2}$	150
108.5	4 Be	K$\alpha_{1,2}$	150
183.3	5 B	K$\alpha_{1,2}$	151
277	6 C	K$\alpha_{1,2}$	147
348.3	21 Sc	Ll	21
392.4	7 N	K$\alpha_{1,2}$	150
395.3	22 Ti	Ll	46
395.4	21 Sc	L$\alpha_{1,2}$	111
399.6	21 Sc	Lβ_1	77
446.5	23 V	Ll	28
452.2	22 Ti	L$\alpha_{1,2}$	111
458.4	22 Ti	Lβ_1	79
500.3	24 Cr	Ll	17
511.3	23 V	L$\alpha_{1,2}$	111
519.2	23 V	Lβ_1	80
524.9	8 O	K$\alpha_{1,2}$	151
556.3	25 Mn	Ll	15
572.8	24 Cr	L$\alpha_{1,2}$	111
582.8	24 Cr	Lβ_1	79
615.2	26 Fe	Ll	10
637.4	25 Mn	L$\alpha_{1,2}$	111
648.8	25 Mn	Lβ_1	77
676.8	9 F	K$\alpha_{1,2}$	148
677.8	27 Co	Ll	10
705.0	26 Fe	L$\alpha_{1,2}$	111
718.5	26 Fe	Lβ_1	66
742.7	28 Ni	Ll	9
776.2	27 Co	L$\alpha_{1,2}$	111
791.4	27 Co	Lβ_1	76
811.1	29 Cu	Ll	8
833	57 La	Mα_1	100
848.6	10 Ne	K$\alpha_{1,2}$	150

⋮

X-ray fluorescence transition lines (cont.)

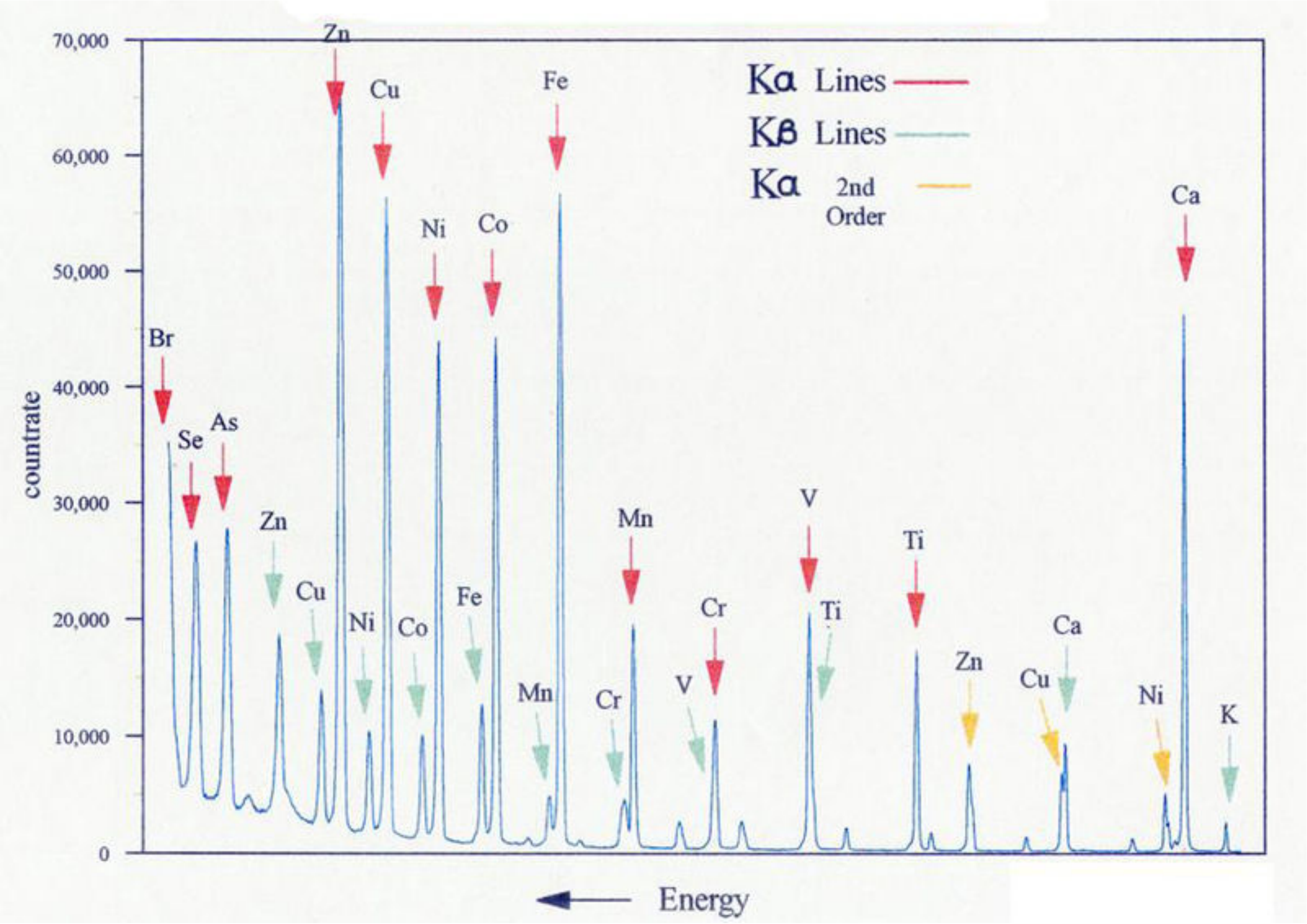

XRF: X-Ray Fluorescence

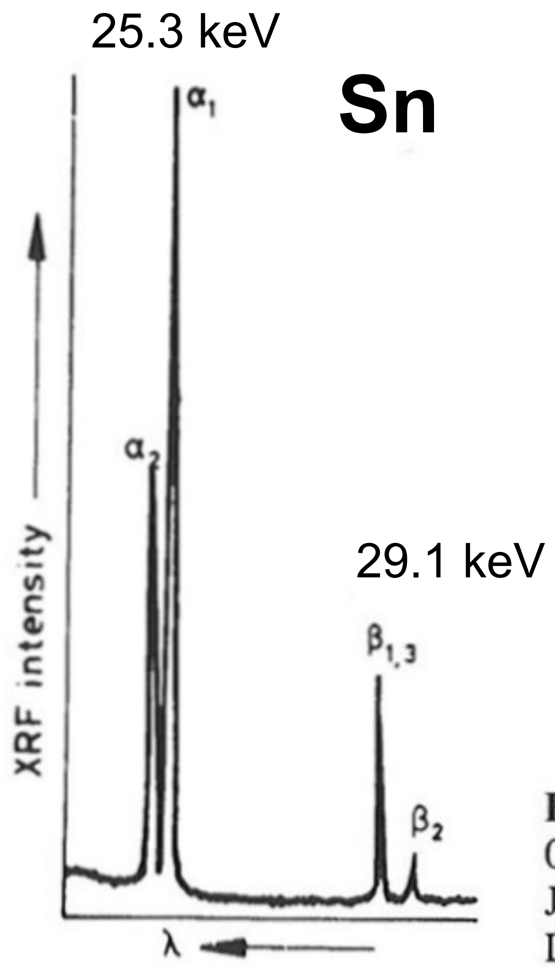

Transition lines

$K\alpha_1 : K_1 - L_3,\ 1s - 2p_{3/2}$

$K\alpha_2 : K_1 - L_2,\ 1s - 2p_{1/2}$

$K\beta_1 : K_1 - M_2,\ 1s - 3p_{1/2}$

$K\beta_2 : K_1 - N_{2,3},\ 1s - 4p_{1/2,3/2}$

$K\beta_3 : K_1 - M_3,\ 1s - 3p_{3/2}$

position: transition energy

intensity: transition rate

Figure 8.30 *K* emission spectrum of tin. The α_1 and β_2 lines are at 0.491 and 0.426 Å, respectively. (Reproduced, with permission, from Jenkins, R., *An Introduction to X-ray Spectrometry*, p. 22, Heyden, London, 1976)

Kα fluorescence: a simple model

- Simple model of an atomic species of atomic number *Z*
  - 1*s* orbital ~ H-like 1*s* orbital of *Z*
  - 2*p* orbital ~ H-like 2*p* orbital of *Z*
- Kα photon energy: $\omega_{K\alpha} \sim Z^2$
- Kα fluorescence rate: $\Gamma_{K\alpha} \sim Z^4$

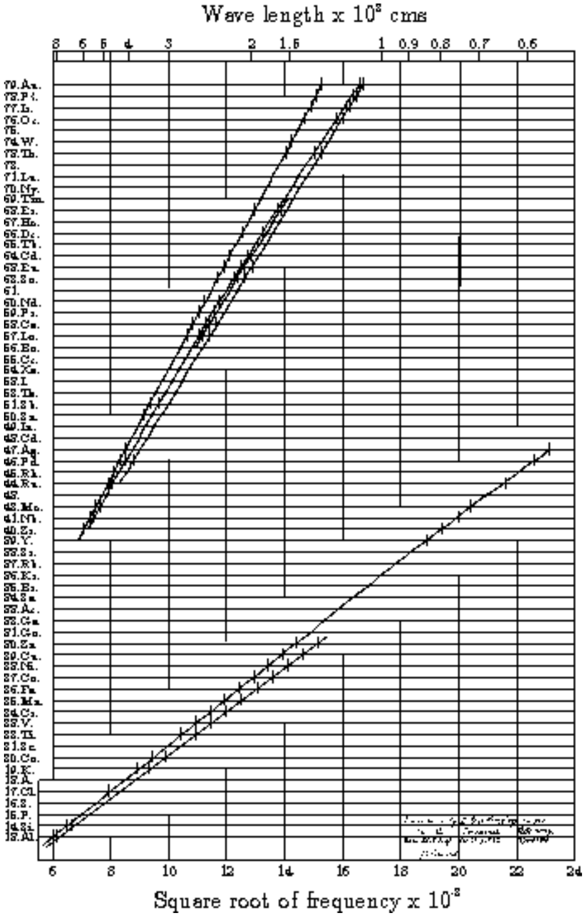

Moseley's law

$$\sqrt{\omega} \propto Z$$

Phil. Mag. **27**, 702 (1914).

Auger-Meitner within mean-field model

A renaming proposal to Auger-Meitner: Physics Today 72, 10 (2019).

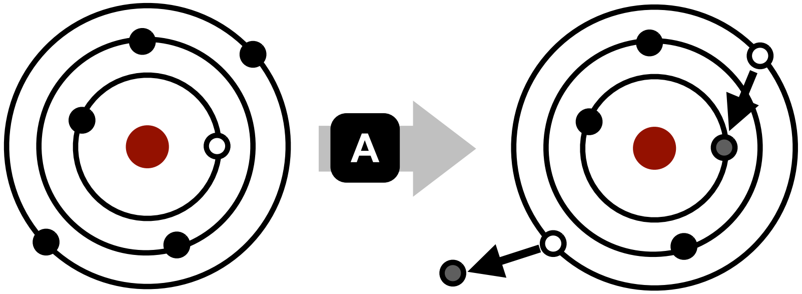

Initial state: $|I\rangle = \hat{c}_i |\Phi_0^{N_\mathrm{el}}\rangle$

Final state: $|F\rangle = \hat{c}_a^\dagger \hat{c}_j \hat{c}_{j'} |\Phi_0^{N_\mathrm{el}}\rangle, \quad j, j' \neq i$

Auger rate: $\Gamma_{FI} = 2\pi\delta(E_F - E_I) \left| \langle F | \hat{H}_\mathrm{int} | I \rangle \right|^2$

Auger-Meitner rate and energy

Perturbation theory $\hat{H}_0 = \hat{F},\ \hat{H}_{\text{int}} = \frac{1}{2}\sum_{pqrs} v_{pqrs}\hat{c}_p^\dagger \hat{c}_q^\dagger \hat{c}_s \hat{c}_r - \sum_{pq}\sum_i \left\{v_{piqi} - v_{piiq}\right\} \hat{c}_p^\dagger \hat{c}_q$

Coulomb matrix element $v_{pqrs} = \int \mathrm{d}^3x \int \mathrm{d}^3x' \varphi_p^\dagger(\boldsymbol{x})\varphi_q^\dagger(\boldsymbol{x}') \frac{1}{|\boldsymbol{x}-\boldsymbol{x}'|}\varphi_r(\boldsymbol{x})\varphi_s(\boldsymbol{x}')$

Partial Auger-Meitner rate

$$\Gamma_{i,jj'} = 2\pi \sum_a \left|v_{aijj'} - v_{aij'j}\right|^2 \delta(\varepsilon_a + I_j + I_{j'} - I_i)$$

Auger-Meitner electron energy $\varepsilon_a = I_i - I_j - I_{j'}$

KLL Auger-Meitner decay: a simple model

- Simple model of an atomic species of atomic number Z
  - 1*s* orbital ~ H-like 1*s* orbital of Z
  - 2*p* orbital ~ H-like 2*p* orbital of Z
  - Auger electron wave function ~ plane wave

- Focus on the channel with two 2*p* holes in the final state

- *KLL* Auger electron *E*: $\varepsilon_{KLL} \sim Z^2$

- *KLL* Auger decay rate: $\Gamma_{KLL} \sim Z^0$

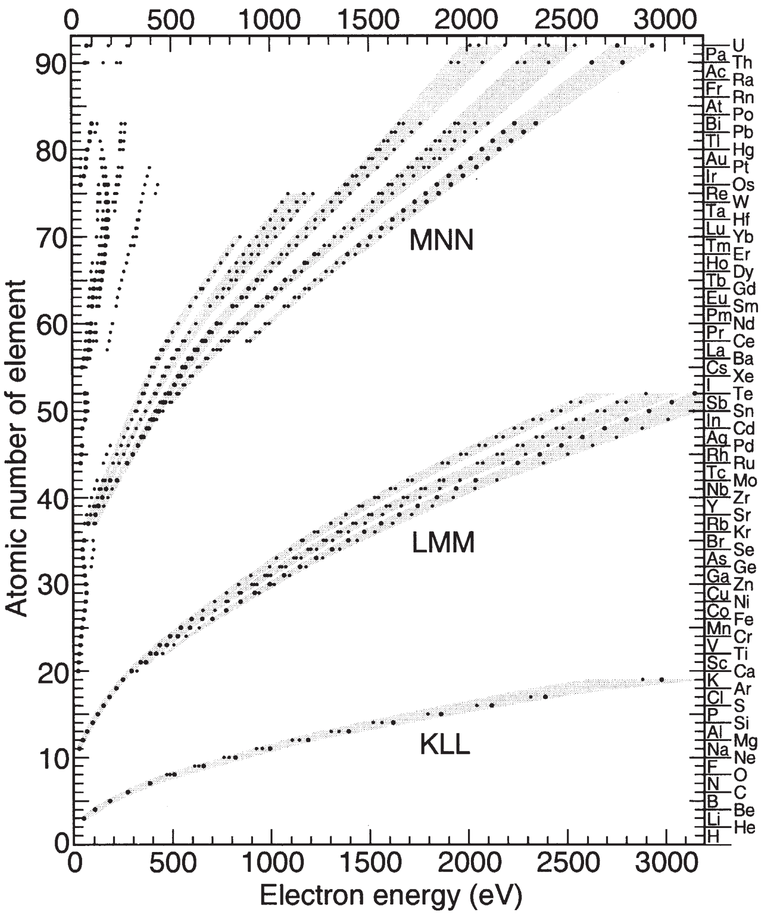

AES: Auger-Meitner Electron Spectrum

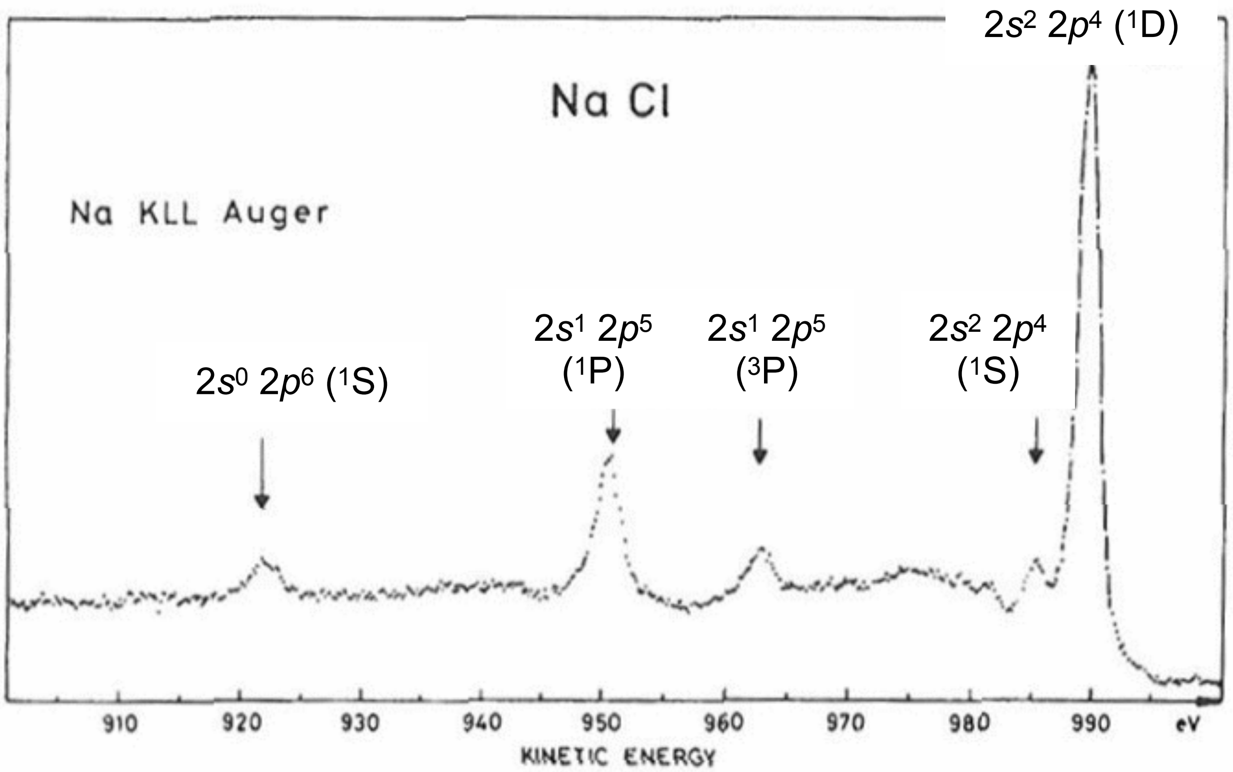

Figure 8.26 The $KL_{\mathrm{II,III}}L_{\mathrm{II,III}}$ ($^1D_2$ and $^1S_0$) Auger spectrum of sodium in solid NaCl. (Reproduced, with permission, from Siegbahn, K. (June 1976), *Publication No. UUIP-940*, p. 81, Uppsala University Institute of Physics)

$$\varepsilon_a = I_i - I_j - I_{j'}$$

Auger-Meitner channels

$1s - 2s\,2s : 2s^0 2p^6$ ^{1}S

$1s - 2s\,2p : 2s^1 2p^5$ ^{1}P

^{3}P

$1s - 2p\,2p : 2s^2 2p^4$ ^{1}S

~~^{3}P~~

^{1}D

position: AM energy

intensity: AM rate

X-ray scattering

Elastic X-ray scattering

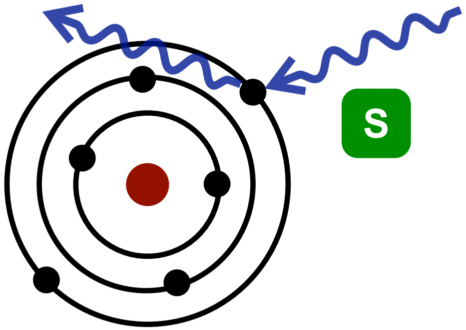

Initial state: $|I\rangle = |\Psi_0^{N_\mathrm{el}}\rangle |N_\mathrm{EM}\rangle$

Final state: $|F\rangle = |\Psi_0^{N_\mathrm{el}}\rangle \hat{a}^\dagger_{\boldsymbol{k}_F,\lambda_F} |N_\mathrm{EM} - 1\rangle$

Scattering rate: $\Gamma_{FI} = 2\pi\delta(E_F - E_I) \left| \langle F|\hat{H}_\mathrm{int}|I\rangle \right|^2$

Elastic X-ray scattering form factor

Transition rate

$$\Gamma_{FI} = \frac{(2\pi)^3}{V}\frac{N_{\mathrm{EM}}}{V}\frac{1}{\omega_F\omega_{\mathrm{in}}}\left|\boldsymbol{\epsilon}^*_{\boldsymbol{k}_F,\lambda_F}\cdot\boldsymbol{\epsilon}_{\boldsymbol{k}_{\mathrm{in}},\lambda_{\mathrm{in}}}\right|^2\left|f^0(\boldsymbol{k}_{\mathrm{in}}-\boldsymbol{k}_F)\right|^2\delta(\omega_F-\omega_{\mathrm{in}})$$

Scattering vector
(or momentum transfer)

$$\boldsymbol{Q} = \boldsymbol{k}_{\mathrm{in}} - \boldsymbol{k}_F$$

Scattering (or form) factor

$$f^0(\boldsymbol{Q}) = \int \mathrm{d}^3x\,\rho^{(\mathrm{el})}(\boldsymbol{x})\mathrm{e}^{\mathrm{i}\boldsymbol{Q}\cdot\boldsymbol{x}}$$

Electron density

$$\rho^{(\mathrm{el})}(\boldsymbol{x}) = \langle\Psi_0^{N_{\mathrm{el}}}|\hat{\psi}^\dagger(\boldsymbol{x})\hat{\psi}(\boldsymbol{x})|\Psi_0^{N_{\mathrm{el}}}\rangle$$

Elastic x-ray scattering cross section

Differential cross section

$$\mathrm{d}\sigma = \sum_{\boldsymbol{k}_F,\lambda_F} \frac{\Gamma_{FI}}{J_{\mathrm{EM}}} = \frac{V}{(2\pi)^3}\alpha^3 \mathrm{d}\Omega \sum_{\lambda_F} \int_0^\infty \mathrm{d}\omega_F\, \omega_F^2 \frac{\Gamma_{FI}}{J_{\mathrm{EM}}}$$

$$\frac{\mathrm{d}\sigma(\boldsymbol{Q})}{\mathrm{d}\Omega} = \alpha^4 \left|f^0(\boldsymbol{Q})\right|^2 \sum_{\lambda_F} \left|\boldsymbol{\epsilon}^*_{\boldsymbol{k}_F,\lambda_F} \cdot \boldsymbol{\epsilon}_{\boldsymbol{k}_{\mathrm{in}},\lambda_{\mathrm{in}}}\right|^2 = \left(\frac{\mathrm{d}\sigma}{\mathrm{d}\Omega}\right)_T \left|f^0(\boldsymbol{Q})\right|^2$$

Total form factor decomposed in terms of atomic contributions

$$\begin{aligned} f^0(\boldsymbol{Q}) &\approx \int \mathrm{d}^3x \sum_n \rho_n^{(\mathrm{el})}(\boldsymbol{x} - \boldsymbol{R}_n)\mathrm{e}^{\mathrm{i}\boldsymbol{Q}\cdot\boldsymbol{x}} \\ &= \sum_n \left\{ \int \mathrm{d}^3x'\, \rho_n^{(\mathrm{el})}(\boldsymbol{x}')\mathrm{e}^{\mathrm{i}\boldsymbol{Q}\cdot\boldsymbol{x}'} \right\} \mathrm{e}^{\mathrm{i}\boldsymbol{Q}\cdot\boldsymbol{R}_n} \\ &\equiv \sum_n f_n^0(\boldsymbol{Q})\mathrm{e}^{\mathrm{i}\boldsymbol{Q}\cdot\boldsymbol{R}_n} \end{aligned}$$

Atomic form factor

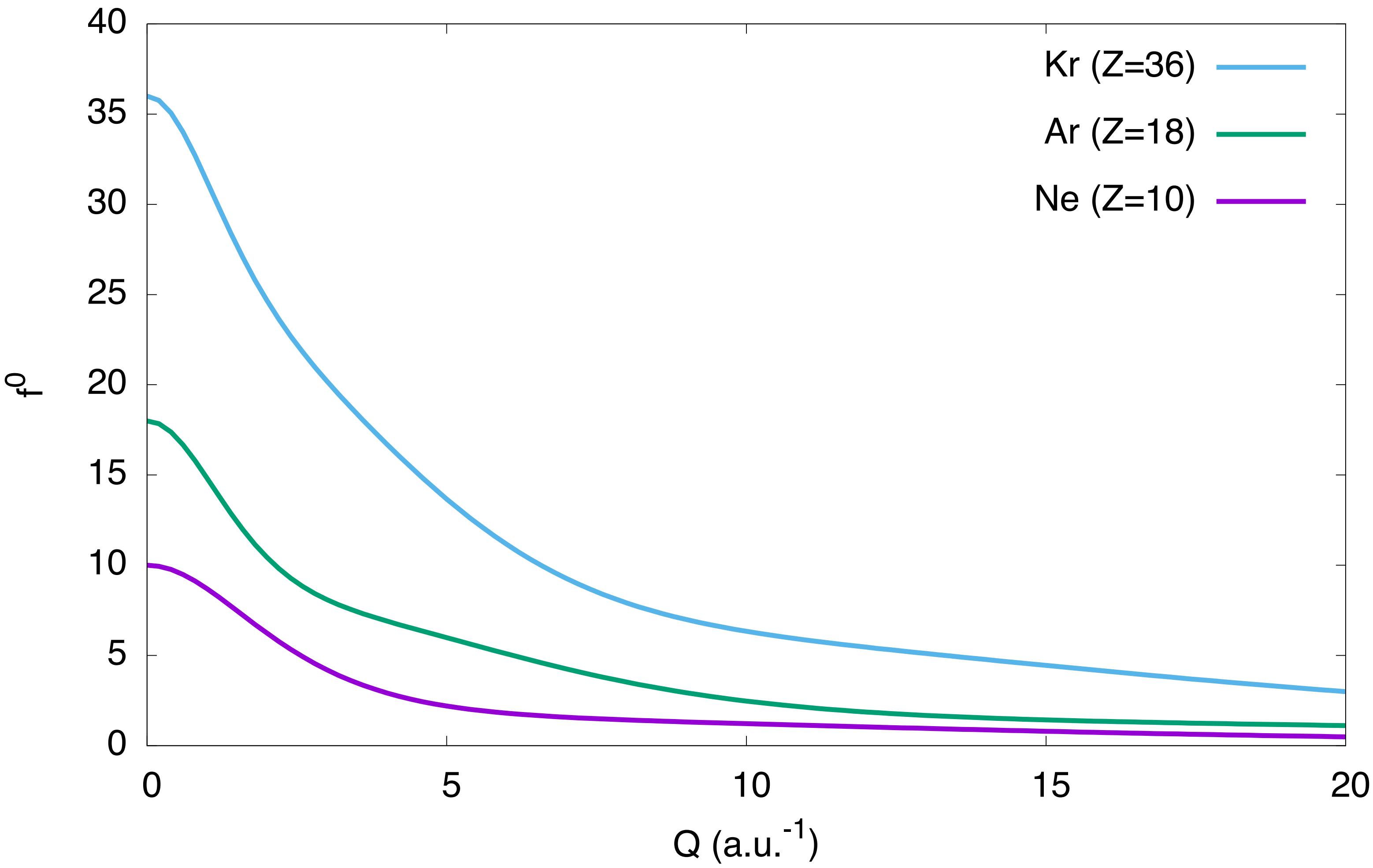

Absorption vs. scattering

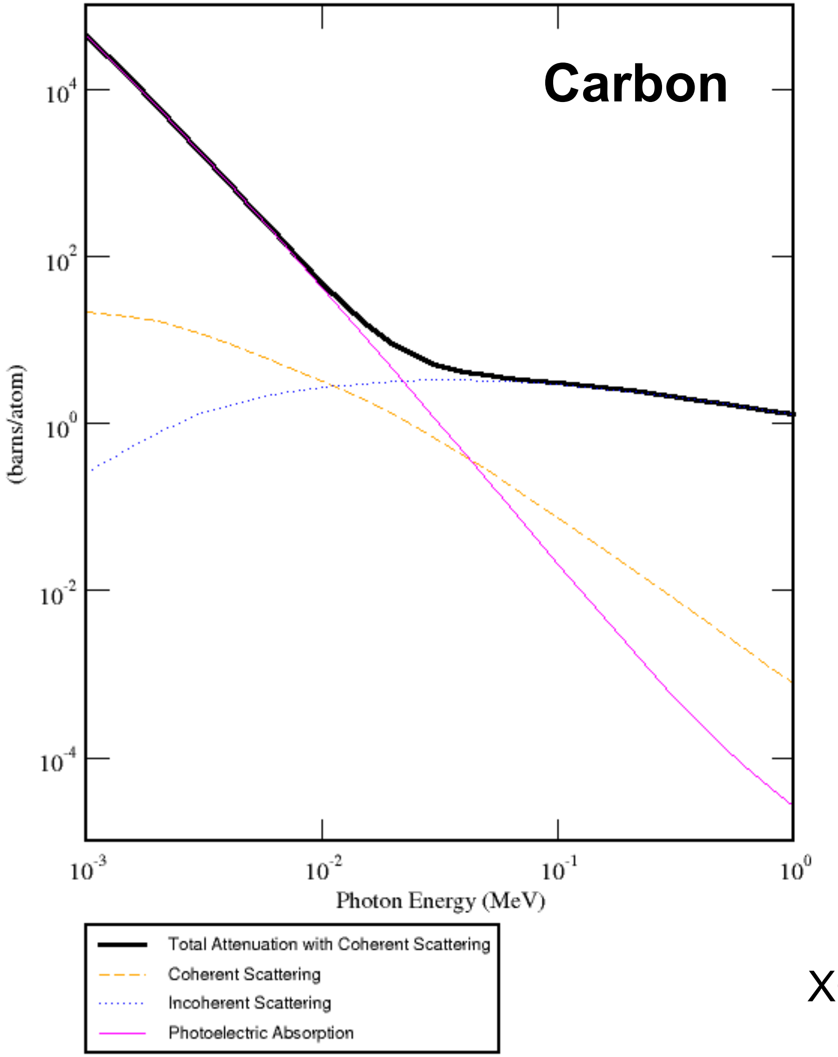

C@10 keV

$\sigma_{\text{absorption}}$=41 barn

$\sigma_{\text{el. scattering}}$=3.2 barn

$\sigma_{\text{inel. scattering}}$=2.7 barn

$$\frac{\sigma_{\text{el. sc}}}{\sigma_{\text{abs}}} \sim \frac{1}{13}$$

XCOM, NIST: https://dx.doi.org/10.18434/T48G6X

Dispersive correction to elastic X-ray scattering

- Resonant elastic x-ray scattering:
  When the photon energy approaches to the ionization potential, the second order of p•A becomes important.

Elastic X-ray scattering tensor: second-order correction with p•A

$$\begin{aligned} f_{i,j}(\boldsymbol{Q},\boldsymbol{k}_{\mathrm{in}}) &= f^0(\boldsymbol{Q})\delta_{i,j} \\ &+ \sum_r \langle \Psi_0^{N_{\mathrm{el}}} | \int \mathrm{d}^3x\, \hat{\psi}^\dagger(\boldsymbol{x}) \mathrm{e}^{-\mathrm{i}\boldsymbol{k}_F\cdot\boldsymbol{x}} \frac{(\boldsymbol{\nabla})_i}{\mathrm{i}} \hat{\psi}(\boldsymbol{x}) | \Psi_r^{N_{\mathrm{el}}} \rangle \\ &\times \frac{1}{E_0^{N_{\mathrm{el}}} + \omega_{\mathrm{in}} - E_r^{N_{\mathrm{el}}} + \mathrm{i}\epsilon} \\ &\times \langle \Psi_r^{N_{\mathrm{el}}} | \int \mathrm{d}^3x\, \hat{\psi}^\dagger(\boldsymbol{x}) \mathrm{e}^{\mathrm{i}\boldsymbol{k}_{\mathrm{in}}\cdot\boldsymbol{x}} \frac{(\boldsymbol{\nabla})_j}{\mathrm{i}} \hat{\psi}(\boldsymbol{x}) | \Psi_0^{N_{\mathrm{el}}} \rangle. \end{aligned}$$

Dispersive correction to elastic X-ray scattering

Elastic X-ray scattering in the forward direction

Scalar scattering factor $f(\omega_{\text{in}}, \boldsymbol{\epsilon}_{\text{in}}) = f^0(\mathbf{0}) + f'(\omega_{\text{in}}, \boldsymbol{\epsilon}_{\text{in}}) + \mathrm{i} f''(\omega_{\text{in}}, \boldsymbol{\epsilon}_{\text{in}})$

Total number of electrons $f^0(\mathbf{0}) = N_{\text{el}}$

Relationship between imaginary part of scattering factor and absorption cross section

$$f''(\omega_{\text{in}}, \boldsymbol{\epsilon}_{\text{in}}) = -\frac{\omega_{\text{in}}}{4\pi\alpha} \sum_F \sigma_F(\omega_{\text{in}}, \boldsymbol{\epsilon}_{\text{in}})$$

Kramers-Kronig relation

$$f'(\omega_{\text{in}}, \boldsymbol{\epsilon}_{\text{in}}) = \frac{1}{\pi} \mathrm{Pr} \int_{-\infty}^{\infty} \mathrm{d}\omega'_{\text{in}} \, \frac{f''(\omega'_{\text{in}}, \boldsymbol{\epsilon}_{\text{in}})}{\omega'_{\text{in}} - \omega_{\text{in}}}$$

Dispersive correction (anomalous scattering)

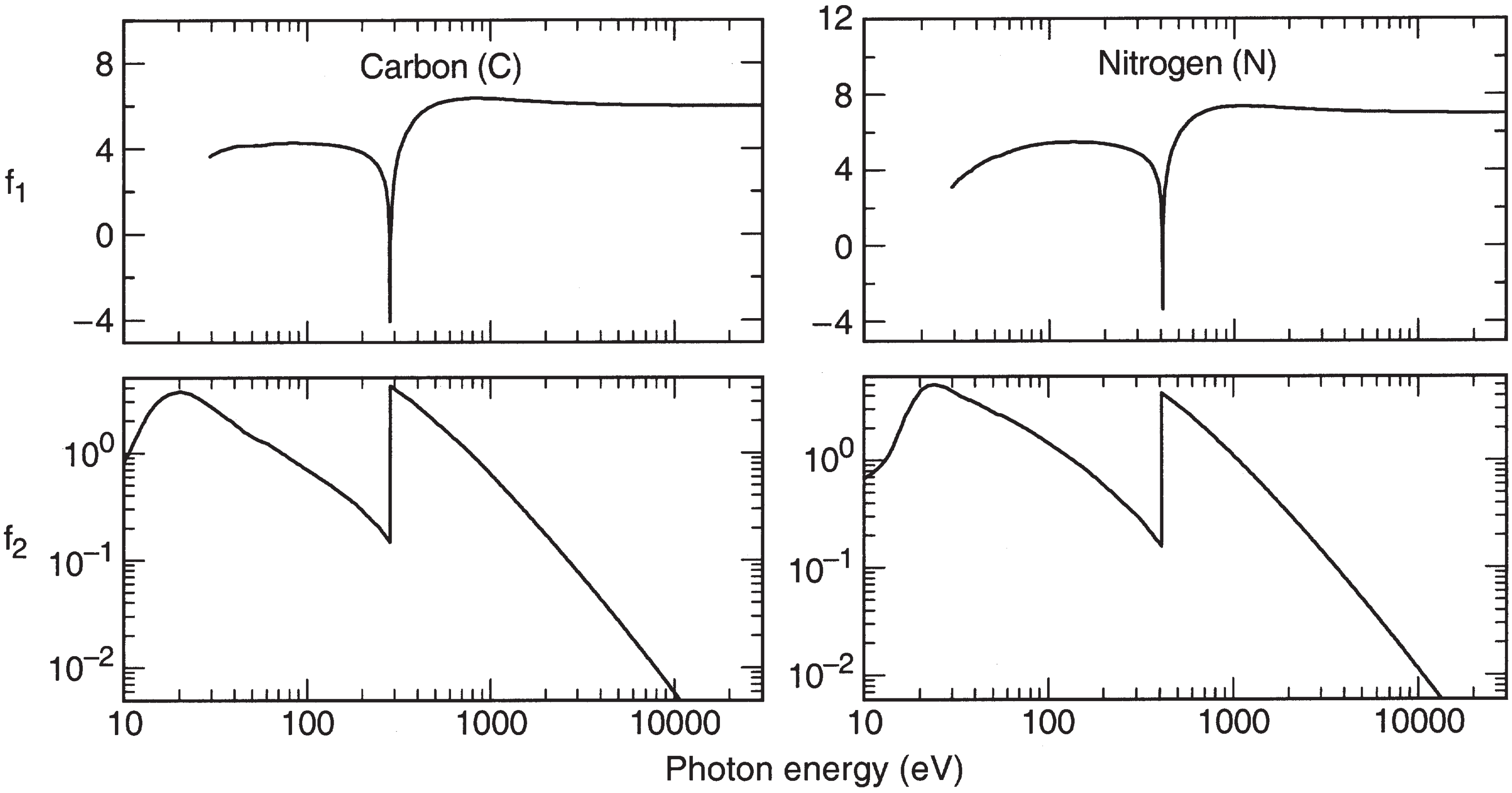

$$f_1 \equiv f^0 + f' \qquad f_2 \equiv -f''$$

X-ray scattering

elastic vs. inelastic

$$|\Psi_I^{\mathrm{el}}\rangle = |\Psi_F^{\mathrm{el}}\rangle \qquad |\Psi_I^{\mathrm{el}}\rangle \neq |\Psi_F^{\mathrm{el}}\rangle$$

without *M* vs. with *M*

(A^2) **(p•A)**

- Elastic X-ray scattering
  - Non-resonant elastic X-ray scattering via A^2
  - Resonant elastic X-ray scattering via p•A (Dispersion correction)
- Inelastic X-ray scattering
  - Non-resonant inelastic X-ray scattering via A^2 (Compton scattering)
  - Resonant inelastic X-ray scattering via p•A (RIXS or resonant X-ray Raman)

X-ray crystallography

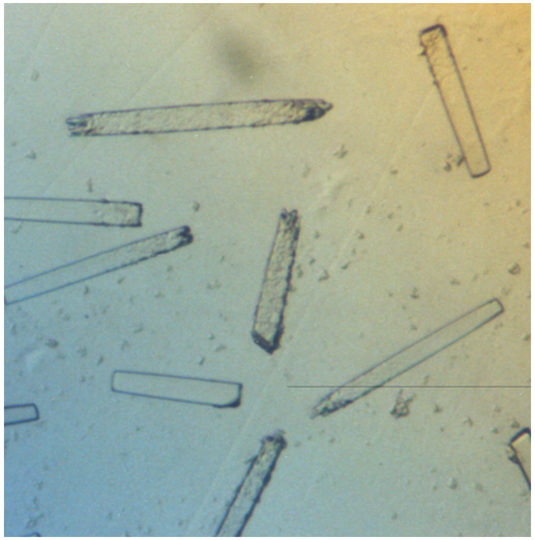

Protein crystal

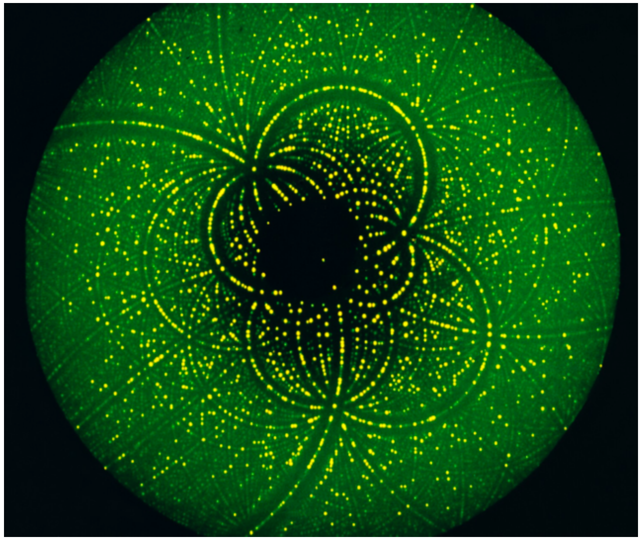

X-ray diffraction pattern

$$I \sim \left| f^0(\boldsymbol{Q}) \right|^2$$

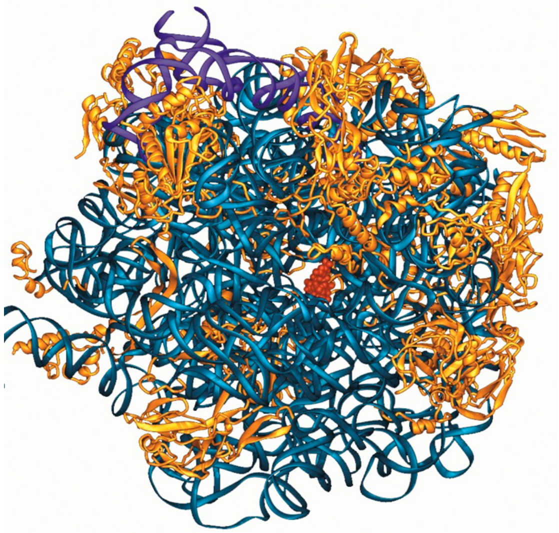

Molecular structure of a protein

$$f^0(\boldsymbol{Q}) \underset{\mathrm{FT}}{\overset{\mathrm{IFT}}{\rightleftarrows}} \rho^{(\mathrm{el})}(\boldsymbol{x})$$

Summary

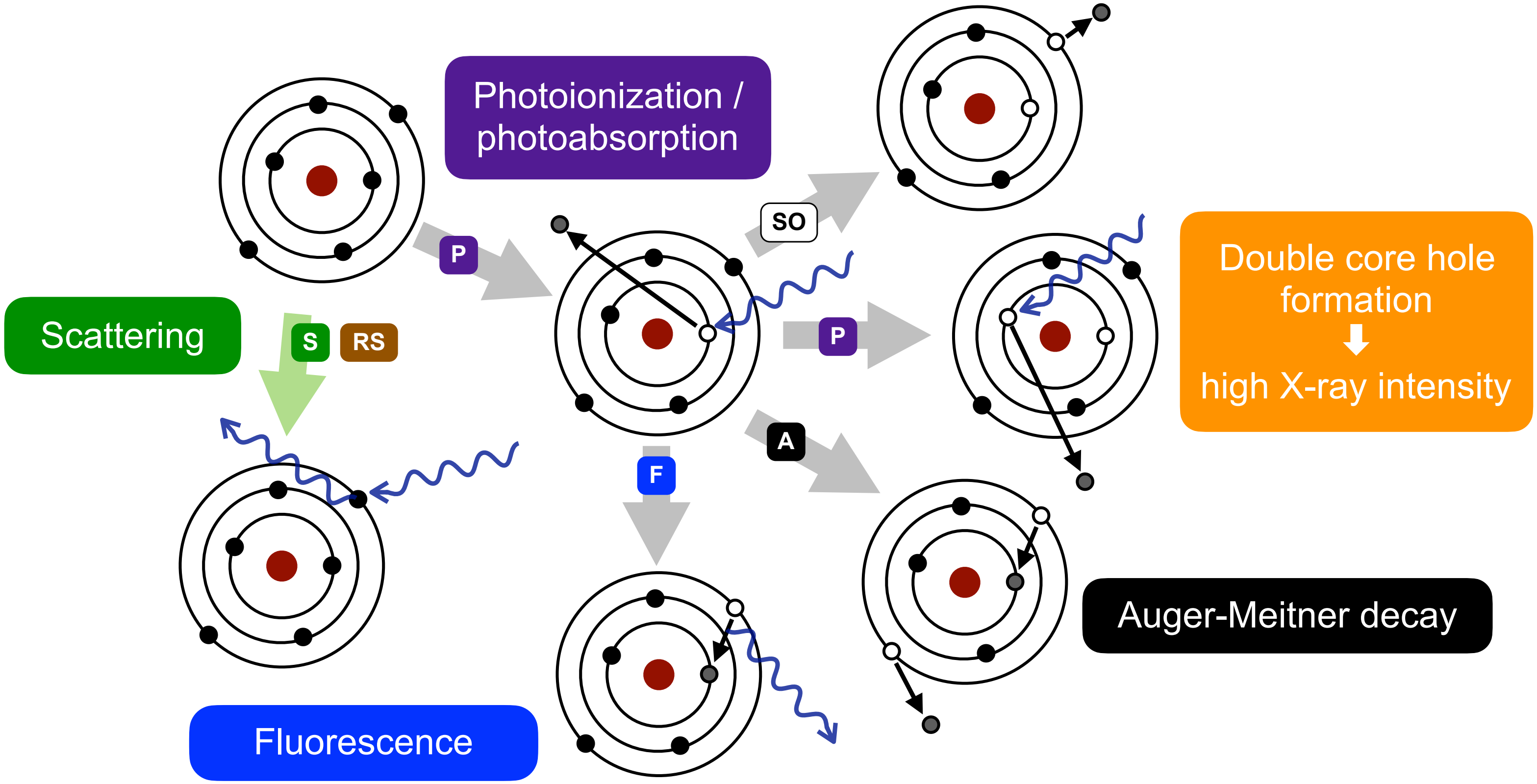

- Theoretical aspects of X-ray-induced processes
- Many-electron system: mean-field approach
- σ and Γ calculated within the same framework (QED and TDPT)

References

- D. Attwood, *Soft x-rays and extreme ultraviolet radiation* (Cambridge University Press).
- J. Als-Nielsen and D. McMorrow, *Elements of Modern X-Ray Physics* (Wiley).
- S. Bare, EXAFS Data Collection and Analysis Workshop, July 14-17, 2003, National Synchrotron Light Source, Brookhaven National Laboratory http://cars9.uchicago.edu/xafs/NSLS_EDCA/July2003/.
- J. M. Hollas, *Modern Spectroscopy* (Wiley).
- F. Reinert and S. Huefner, Photoemission spectroscopy—from early days to recent applications, *New Journal of Physics* **7**, 97 (2005).
- R. Santra, Concepts in x-ray physics, *Journal of Physics B* **42**, 023001 (2009).
- R. Santra *et al.*, Strong-field control of x-ray processes, *Advances in Atomic, Molecular, and Optical Physics* **56**, 219 (2008).
- J. Stoehr, *NEXAFS Spectroscopy* (Springer).
- A. C. Thompson and D. Vaughan, *X-ray data booklet*, Center for X-Ray Optics and Advanced Light Source, Lawrence Berkeley National Laboratory http://xdb.lbl.gov/.
- Z. Jurek, S.-K. Son, *et al.*, XMDYN and XATOM, *J. Appl. Cryst.* **49**, 1048 (2016).

Computer simulations with XATOM

Let’s go with neon!

- Let’s calculate electronic structure of Ne
- Let’s calculate photoionization cross section of Ne at 2 keV

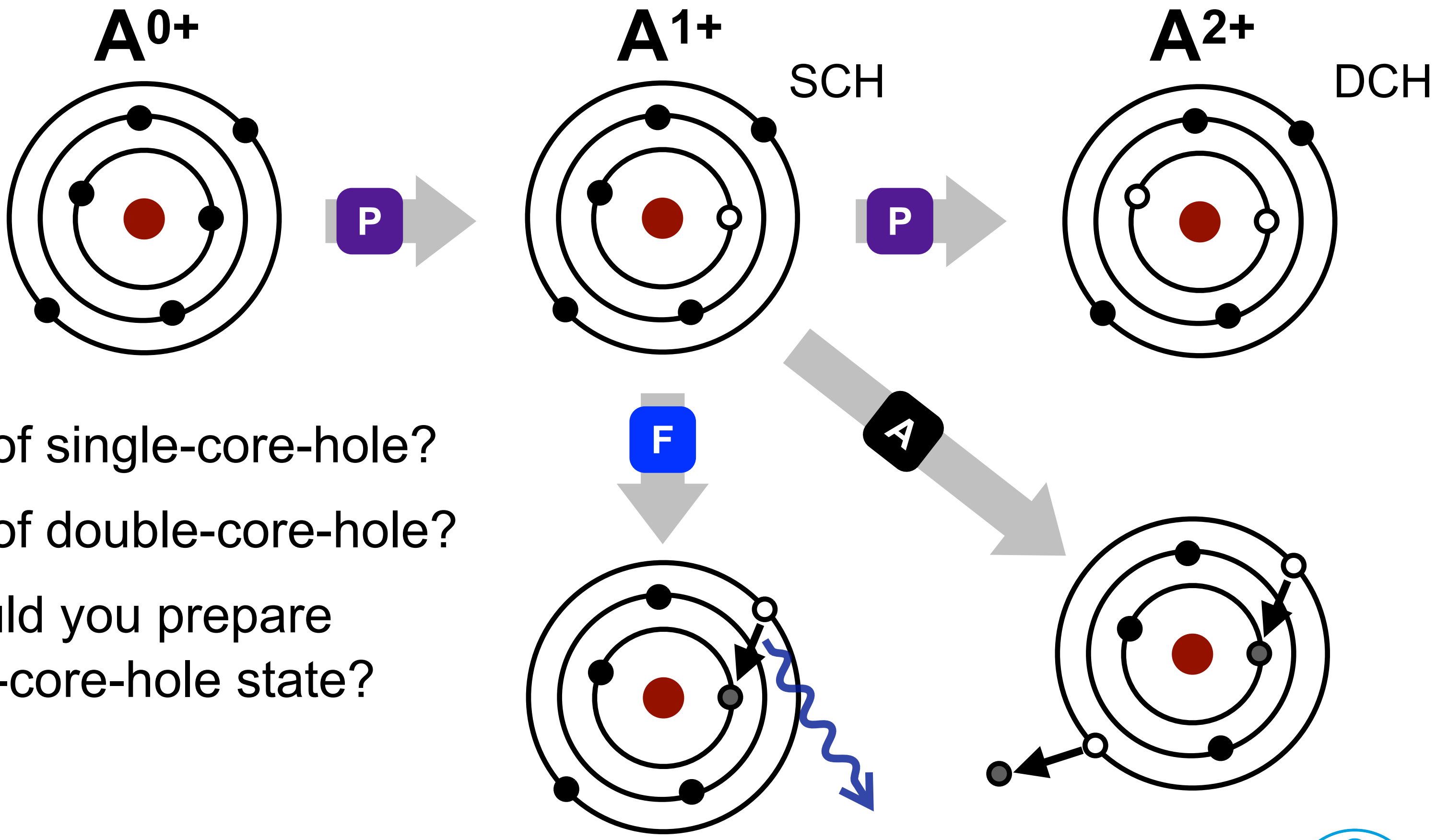

- Lifetime of single-core-hole?
- Lifetime of double-core-hole?
- How would you prepare a double-core-hole state?